



MARMARA UNIVERSITY
INSTITUTE FOR GRADUATE STUDIES
IN PURE AND APPLIED SCIENCES



NUMERICAL AND EXPERIMENTAL
INVESTIGATION OF A DOMESTIC NATURAL
GAS BURNER AND ANALYSIS OF
MODIFICATIONS TO ACHIEVE LOW NOX
EMISSIONS

ENGİN UZA

MASTER THESIS

Department of Mechanical Engineering

Thesis Supervisor

Yrd. Doç. Dr. Barış YILMAZ

ISTANBUL, 2017



MARMARA UNIVERSITY
INSTITUTE FOR GRADUATE STUDIES
IN PURE AND APPLIED SCIENCES



NUMERICAL AND EXPERIMENTAL
INVESTIGATION OF A DOMESTIC NATURAL
GAS BURNER AND ANALYSIS OF
MODIFICATIONS TO ACHIEVE LOW NOX
EMISSIONS

ENGİN UZA

524612023

MASTER THESIS

Department of Mechanical Engineering

Thesis Supervisor

Yrd. Doç. Dr. Barış YILMAZ

ISTANBUL, 2017

**MARMARA UNIVERSITY INSTITUTE
FOR GRADUATE STUDIES IN PURE AND
APPLIED SCIENCES**

Engin UZA a Master of Science of Mechanical Engineering student of Marmara University Institute for Graduate Studies in Pure and Applied Sciences, defended his thesis entitled “**Numerical and Experimental Investigation of a Domestic Natural Gas Burner and Analysis of Modifications to Achieve Low NOx Emissions**”, on and has been found to be satisfactory by the jury members.

Jury Members

Assist. Prof. Barış YILMAZ (Advisor)

Marmara University(SIGN).....

Prof. Uner COLAK (Jury Member)

Istanbul Technical University(SIGN).....

Assist. Prof. Mustafa YILMAZ (Jury Member)

Marmara University(SIGN).....

APPROVAL

Marmara University Institute for Graduate Studies in Pure and Applied Sciences Executive Committee approves that Engin UZA be granted the degree of Master of Science of Mechanical Engineering in Department of Mechanical Engineering, Mechanical Engineering Program on 29.05.2017 (Resolution no: 2017/13.02)

Director of the Institute

Prof. Dr. Uğur YAHŞİ

ACKNOWLEDGEMENT

I would like to thank my academic supervisor Assist. Prof. Barış Yılmaz for his guidance and support sharing his knowledge and ideas with me.

I would like to thank all my professors and friends in Mechanical Engineering Department of Marmara University.

I would like to specially thanks to İhsan Bayraklı for sharing his knowledge, experiences about combustion systems and life.

I would like to thank General Manager of Ecostar Combustion Systems Cem Özyıldırım, Factory Manager Emir F. Sakallı, all my colleagues especially G.Akgün, E.Bingöl, A.Tezcan, Ö.Kayhan, O.Salcı and ECOSTAR Combustion Systems for their support during my thesis study and experiments.

My warmest gratitude goes to my deceased father Mustafa Adnan Uza, my mother Asuman Uza and Nihal Şimşek, the study could never have been done without the support and encouragement from you.

A special thank goes to an angel who come to my life and made my life awesome. Special thanks to her patience and endless support.

APRIL 2017

Engin UZA

CONTENTS

ACKNOWLEDGEMENT	i
CONTENTS	ii
ÖZET	iv
ABSTRACT	v
CLAIM FOR ORIGINALITY	vi
SYMBOLS	vii
GREEK SYMBOLS	viii
ABBREVIATIONS	ix
LIST OF FIGURES	x
1. INTRODUCTION	1
1.1 Combustion	1
1.1.1 Combustion Types	1
1.1.2 Calorific Value	2
1.2 Burner	3
1.2.1 Burner Types	4
1.3 Combustion Stoichiometry and Combustion Products	7
1.4 Combustion Products	9
1.4.1 Carbon Dioxide	10
1.4.2 Oxygen	10
1.4.3 Carbon Monoxide	10
1.4.4 Nitric Oxides (NO _x)	11
1.4.4.1 NO _x Mechanisms	11
1.4.4.2 NO _x Reduction Techniques	13
1.4.4.3 CO and NO _x Limits and Regulations	16
1.5 Literature Review	16
2. MATERIAL and METHOD	21
2.1 Experimental Setup	21
2.1.1 Test Setup	21
2.1.2 Combustion Chamber Technical Specifications	22
2.1.3 Measurement Devices	24
2.1.4 Burner Technical Specifications	25

2.1.5	Fuel Composition	26
2.2	Numerical Methods	27
2.3	Governing Equations	28
2.4	Combustion Models.....	28
3.	RESULTS and DISCUSSION.....	31
3.1	Experimental Studies.....	31
3.2	Numerical Studies.....	37
3.2.1	Theoretical Air and Combustion Products Calculations	37
3.2.2	Geometry	40
3.2.3	Mesh Independency and Cold Flow Studies	43
3.2.4	Boundary Conditions.....	46
3.2.5	Reactive Analysis	49
3.2.6	Comparison of Numerical and Experimental Studies	55
3.2.7	Geometry Modifications to Achieve Low NO _x Emission.....	59
4.	CONCLUSIONS.....	65
	REFERENCES.....	67
	CURRICULUM VITAE	71

ÖZET

Bir Doğal Gaz Yakıcısının Nümerik ve Deneysel Araştırılması ve Düşük NO_x Emisyonu Hedefiyle Yapılacak Değişikliklerin Analizi

Hesaplamalı akışkan dinamikleri (CFD), yeni veya mevcut tasarımı optimize etmek için etkili bir araçtır. Tasarlama döngüsü sırasında CFD'nin kullanılması, endüstriyel ürün geliştirme ve akademik araştırmalarda doğru tahmin yapılabilir, tasarım süresini kısaltabilir ve ürün geliştirme maliyetlerini düşürebilir.

Bu tez çalışmasında, ECO-45 endüstriyel ölçekli gaz brülörünün nümerik olarak incelenmiş ve TSE EN 676:2000 standardında tanımlı olan 3. Sınıf 80 mg/kWh'den düşük NO_x emisyon değerlerine sahip dizayn yapılması amacıyla nümerik analiz çalışmaları yapılmıştır.

Soğuk akış için sayısal çalışmalar yapılmıştır. Bu çalışmalarda farklı meshler karşılaştırarak uygun olan mesh sayısı ve mesh boyutu belirlenmiştir. Ardından belirlenen bu mesh ile reaktif analiz çalışmaları yapılmıştır. Modelleme çalışmalarında, sıcaklık, akış alanları ve farklı geometriler için emisyon değerleri hesaplanmıştır. Reaktif analiz çalışmalarında yapılan 11 case çalışmasında iki farklı kazan geometrisi ve üç farklı brülör geometrisi kullanılmıştır. Reaktif çalışmalarda, yanma emisyonlarının mol fraksiyonları, (NO_x, CO₂, O₂) ve statik sıcaklıkları konturları ile incelenmiştir. Farklı hava fazlalık oranları ve brülör yükleri için çalışmalar yapılmıştır.

Nümerik simülasyonları doğrulanması için yapılan deneysel çalışmalar ECOSTAR Yakma Sistemleri laboratuvarının mevcut imkanları kullanılarak gerçekleştirilmiştir.

ABSTRACT

Numerical and Experimental Investigation of a Domestic Natural Gas Burner and Analysis of Modifications to Achieve Low NO_x Emissions

The computational fluid dynamics (CFD) is an effective tool to optimize new or current design. Using CFD during the design cycle, makes accurate prediction, shorten design time and reduce product development cost in industrial product development and academic researches.

In this thesis study, an industrial scale gas burner, namely ECO-45, was investigated numerically for the contribution to the design of a low NO_x gas burner satisfying standards defined in TSE EN 676:2000 Class-3 and having NO_x level of less than 80 mg/kWh.

The numerical studies have been performed initially for cold flow field. The accurate enough mesh number and size have been determined by comparing mesh cases. Then reactive cases have been computed with this mesh. In modelling studies, the temperature and flow fields have been computed and emission levels were calculated for different geometries. In reactive case studies, two different boiler geometries and three different burner geometry have been tried in 11 case studies. The results of reactive studies were examined in terms of contour plots including mole fractions of the emissions (NO_x, CO₂, O₂) and static temperatures. Several equivalence ratios and loads were studied.

The numerical model was verified and validated with available experimental measurements, including emission levels at the exit of the combustion chamber at the test facilities in ECOSTAR company.

CLAIM FOR ORIGINALITY

In this study, ECO-45 modulating gas burner was numerically modelled. Modelled burner tests performed in different combustion chamber setups. The numerical computations were verified with data set obtained from experiment setups.

Similar studies have been performed with various simulation programs on different experimental setups and burner geometry. However, these experimental setups have been numerically modelled first time in this study and this is the first numerical study with ECO series burner.

SYMBOLS

Da	: Damköhler number
g	: Gravity
H_w	: Heat of vaporization of water
k	: Turbulent kinetic energy
n_{H₂O out}	: Moles of water vaporized
n_{fuel in}	: Moles of fuel combusted
R_{slow}	: Slowest reaction rate
T	: Temperature
T_{ad}	: Adiabatic Temperature
U	: Flow velocity

GREEK SYMBOLS

\mathbf{E} : Turbulent dissipation rate

$\mathbf{\Phi}$: Equivalence ratio

λ : Lambda

ρ_{ad} : Adiabatic flame density

ABBREVIATIONS

CFD	: Computational fluid dynamics
EFGR	: External flue gas recirculation
FCC	: First combustion chamber
HHV	: Higher heating value
HVAC	: Heating, ventilation and air conditioning
IFGR	: Internal flue gas recirculation
LHV	: Lower heating value
MV	: Measured value
NG-1	: New Geometry-1
NG-2	: New Geometry-2
PDF	: Probability Density Function
ppmv	: Parts per million volume
SCC	: Second combustion chamber

LIST OF FIGURES

Figure 1.1: Combustion Types	2
Figure 1.2: Premixed and Non-premixed burner	4
Figure 1.3: Atmospheric burner	5
Figure 1.4: Monoblock and Duoblock Burner	6
Figure 1.5: Excess air- flue gas products	8
Figure 1.6: Lambda- flame temperature.....	9
Figure 1.7: Fossil Fuel Combustion and Combustion Products.....	9
Figure 1.8: Combustion products (%) – Lambda.....	11
Figure 1.9: Prompt-Fenimore NO _x formation.....	12
Figure 1.10: Fuel NO _x formation	13
Figure 1.11: External flue gas recirculation	14
Figure 1.12: Internal flue gas recirculation	14
Figure 1.13: Stage combustion.....	15
Figure 1.14: Premixed combustion	15
Figure 2.1: ECOSTAR R&D Laboratory.....	21
Figure 2.2: Dimensions of the FCC and SCC	22
Figure 2.3: Flow Diagram of the ECOSTAR R&D Laboratory	23
Figure 2.4: ECO-45 Gas Burner Equipment's	26
Figure 2.5: Fuel Composition (%).....	26
Figure 2.6: Combustion Phenomenology and Combustion Modelling.....	29
Figure 3.1: Test setup-1 (FCC)	31
Figure 3.2: Test setup and measured operating parameters of the	31
Figure 3.3: Test setup-2 (SCC)	32
Figure 3.4: Test setup and measured operating parameters of the SCC	32
Figure 3.5: Lambda versus oxygen percentage [%]	33
Figure 3.6: Lambda versus carbon monoxide [ppm]	34
Figure 3.7: Lambda versus carbon dioxide percentage [%].....	34
Figure 3.8: Lambda versus nitrogen oxide [ppm]	34

Figure 3.9: Gas consumption [Nm ³ /h] versus oxygen percentage [%]	35
Figure 3.10: Gas consumption [Nm ³ /h] versus ca carbon dioxide [%].....	35
Figure 3.11: Gas consumption [Nm ³ /h] versus nitrogen oxide [ppm]	36
Figure 3.12: Thermal camera image of the combustion chamber during the experiments	36
Figure 3.13: Thermal camera image of the flue part during the experiments	37
Figure 3.14: Burner geometry and CFD burner geometry	41
Figure 3.15: Geometry-1	41
Figure 3.16: Geometry-2	41
Figure 3.17: Imported first burner and boiler geometry.....	42
Figure 3.18: Fluid volume of numerical studies of the burner geometry.....	42
Figure 3.19: Fluid volume of numerical studies of the first geometry.....	42
Figure 3.20: Imported second burner and boiler geometry	43
Figure 3.21: Fluid volume of numerical studies of the second geometry	43
Figure 3.22: Axial Velocity [m/s] versus position [m]	44
Figure 3.23: Details of Mesh-3 for the first geometry	45
Figure 3.24: Details of Mesh-3 for the first geometry	45
Figure 3.25: Mesh details of the second geometry.....	46
Figure 3.26: Named selection of boundary conditions for the first geometry	46
Figure 3.27: Named selection of boundary conditions for the second geometry.....	47
Figure 3.28: Temperature [K] contour plots of the first geometry for NG and Methane	50
Figure 3.29: CO ₂ [%] contour plots of the first geometry for NG and Methane	50
Figure 3.30: O ₂ [%] contour plots of the first geometry for NG and Methane.....	50
Figure 3.31: NO _x [ppm] contour plot of the first geometry for NG and Methane	51
Figure 3.32: Contour plots of the numerical study results for the first geometry	51
Figure 3.33: Contour plots of the numerical study results for the first geometry	52
Figure 3.34: Temperature [K] contour plot of the second geometry.....	54
Figure 3.35: CO ₂ [%] contour plot of the second geometry	54
Figure 3.36: O ₂ [%] contour plot of the second geometry.....	54
Figure 3.37: NO _x [ppm] contour plot of the second geometry	55
Figure 3.38: Lambda versus oxygen [%]	56

Figure 3.39: Lambda versus carbon dioxide [%]	56
Figure 3.40: Lambda versus nitrogen oxide [ppm]	57
Figure 3.41: Gas consumption [Nm ³] versus oxygen [%].....	58
Figure 3.42: Gas consumption [Nm ³] versus carbon dioxide [%]	58
Figure 3.43: Gas consumption [Nm ³] versus nitrogen oxide [ppm]	58
Figure 3.44: New Geometry-1	59
Figure 3.45: Temperature contour of New Geometry-1.....	60
Figure 3.46: New Geometry-2	60
Figure 3.47: Mesh details of the NG-2 burner part	61
Figure 3.48: Mesh details of the NG-2.....	61
Figure 3.49: Temperature [K] contour plot of the NG-2.....	62
Figure 3.50: CO ₂ [%] contour plot of the NG-2.....	62
Figure 3.51: O ₂ [%] contour plot of the NG-2.....	63
Figure 3.52: NO _x [ppm] contour plot of the second geometry	63

LIST OF TABLES

Table 1.1: LHV and HHV of common fuels	3
Table 1.2: Burner Types.....	4
Table 1.3: Common emission values for a fan assisted burners	10
Table 1.4: EN 676:2008 NO _x Limitations-Emission Class.....	16
Table 1.5: Conversion of the NO _x and CO emissions for natural gas	16
Table 2.1: Measurement Devices	24
Table 2.2: Burner General Specifications	25
Table 2.3: Burner Technical Specifications	25
Table 3.1: Test conditions for the experimental studies in FCC.....	33
Table 3.2: Emission test values for 125.1 Nm ³ /h gas consumption.....	33
Table 3.3: Emission test values for $\lambda=1.2$ in different burner loads	35
Table 3.4: Emission test values and test conditions of the second experiment.....	36
Table 3.5: Natural gas density calculation results for 100% Methane.....	38
Table 3.6: Theoretical combustion products calculations of 100% Methane, $\lambda = 1$	38
Table 3.7: Theoretical combustion products calculations of 100% Methane, $\lambda = 1.2$	38
Table 3.8: Natural gas composition.....	39
Table 3.9: Natural gas density calculation for natural gas mixture.....	39
Table 3.10: Theoretical combustion products calculations of natural gas mixture, $\lambda = 1$	39
Table 3.11: Theoretical combustion products calculations of mixed NG, $\lambda = 1.2$	40
Table 3.12: Mesh element number and mesh quality of the first geometry.....	44
Table 3.13: Cold flow analysis studies solution conditions	44
Table 3.14: Mesh element number and mesh quality of the second geometry	45
Table 3.15: LHV and HHV calculations of mix natural gas	47
Table 3.16: Mass flow inlet of the fuel and air boundary condition calculations for %100 CH ₄ and mix natural gas combustion.....	48
Table 3.17: Calculated hydraulic diameter for the fuel and air mass flow inlet boundary conditions	48
Table 3.18: Reactive analysis results for the mixed natural gas and %100 methane for 125.1 Nm ³ /h gas consumption in different excess air values for the first geometry.....	49

Table 3.19: Reactive analysis results for the mix natural gas for $\lambda=1.2$ for the first geometry.	53
Table 3.20: Reactive analysis results for the mix natural gas in 35 Nm ³ /h gas consumption for the second geometry in $\lambda=1.3$	53
Table 3.21: Numerical studies and experimental studies comparison of the first reactive analysis case studies and experiments.....	55
Table 3.22: Numerical studies and experimental studies comparison of the second reactive analysis case studies and experiments.....	57
Table 3.23: Numerical studies and experimental studies comparison for the second geometry	59
Table 3.24: Reactive analysis results for the mix natural gas in 125.1 Nm ³ /h gas consumption for the NG-2 in $\lambda=1.2$	61

1. INTRODUCTION

1.1 Combustion

Steady increase of energy consumption causes to increase fossil fuels usage in energy production and that causes unpleasant effect to human beings and the environment. The use of energy more efficiently and the decrease of flue gas emissions are the most important topics in science and engineering recently.

Combustion is the controlled exothermic chemical reaction which provides heat and energy as a result of the reaction between fuel and oxidizer. Nowadays, most of the energy production is still being done by using fossil fuels which are made up ancient, decomposed organic materials. For starting combustion process, fuels need an oxidizer and an ignition source. [1-3]

The fuels in the power generation in industrial applications are almost hydrocarbons (C_xH_y). Hydrocarbons are organic compounds consisting carbon and hydrogen in their molecular structure. Hydrocarbons can be found in the form of gases, liquids, and solids. [1-5]

The aim of this study is to investigate natural gas combustion in an industrial scale gas burner. Therefore, the gas combustion will be considered in detail in the next parts of the thesis.

1.1.1 Combustion Types

Combustion is classified according to how the fuel and oxidant are mixed. It is classified into three main categories which are non-premixed, partially premixed and premixed combustion. Schematic drawings of combustion types are shown in **Figure 1.1**.

Non-premixed (diffusion) combustion, fuel and oxidizer are separated and unmixed before the combustion begins. In this mode of combustion, the flame is called non-premixed or diffusion flames. These types of flames are longer and have lower hot spot temperature than premixed flames. [1]

Premixed flame (combustion), fuel and oxidizer are mixed before the combustion. Premixed flames are shorter and more intense compared to partially premixed and non-premixed flames. [1]

Partially premixed flame (combustion), some fraction of fuel and oxidizer is mixed before combustion begins. Partially premixed flames have a flame length and temperature distribution between premixed and non-premixed flames. [1]

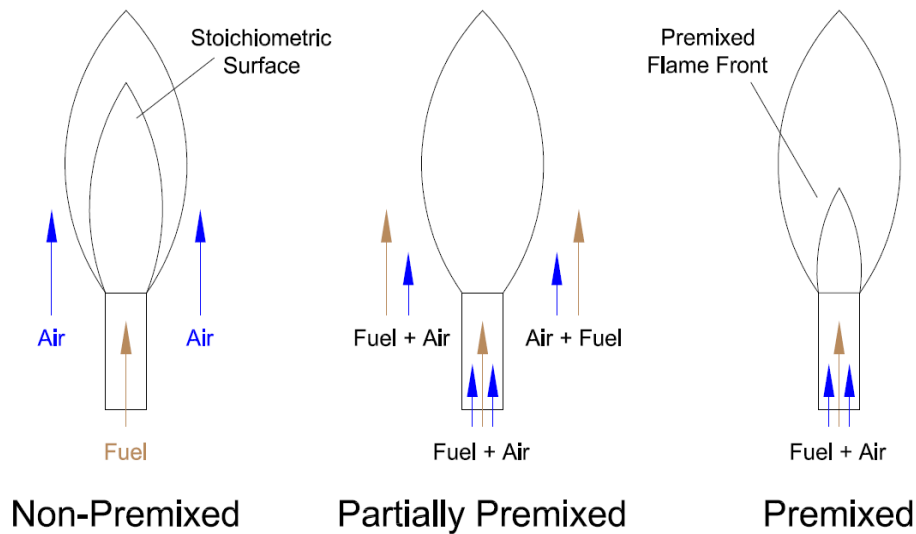


Figure 1.1: Combustion Types

1.1.2 Calorific Value

Calorific value of the fuel is the thermal energy released in combustion, for 1 kg of liquid fuel in liquid fuels, for 1 Nm³ of gas in gaseous fuels. There are two types of heating values depending on the phase of the water in the flue gases.

Lower heating value (LHV) is the amount of heat is released during combustion process assuming the water content of a combustion process is in vapor state at the end of combustion. [1-2]

Higher heating value (HHV), assumes that all the water in a combustion process is in a liquid state after a combustion process. It is obtained such that all products of the combustion are cooled down to the temperature before the combustion. [1-2]

Equation for relating HHV to LHV is; [1]

$$\text{HHV} = \text{LHV} + H_w \left(\frac{n_{\text{H}_2\text{O out}}}{n_{\text{fuel in}}} \right) \quad (1.1)$$

H_w ; Heat of vaporization of water

$n_{\text{H}_2\text{O out}}$; Moles of water vaporized

$n_{\text{fuel in}}$; Moles of fuel combusted

Heating values may be provided in a volume basis, such as kcal/Nm³ or in a mass basis such as kcal/kg. Heating values vary according to the fuel composition and type. LHV and HHV of common fuels are shown in **Table 1.1. [1-2]**

Table 1.1: LHV and HHV of common fuels

Fuel	Unit	HHV	LHV
Natural Gas	kcal/Nm ³	9155	8200
LPG	kcal/kg	11800	10600
Heavy Oil	kcal/kg	10100	9400
Light Oil	kcal/kg	10900	10100
Lignite	kcal/kg	5100	4800
Wood	kcal/kg	3800	3400

1.2 Burner

Burner is a device to provide heat energy to a system by the controlled combustion process. They are designed to provide controlled heat generation by adjusting fuel/oxidant ratio considering the energy demand of a process. In addition, the safe combustion by control of the capacity, ignition period, flame shape and emissions are also satisfied by use of burners.

In most cases, burners use air to oxidize and initiate exothermic chemical reaction. Air is the cheapest oxidant without any storage risk and cost. Pure oxygen can also be used instead of air as an oxidant. However, higher flame temperature is being possible by using pure oxygen due to the lack of nitrogen. The safety of the system and materials should be considered when oxygen is used as an oxidant.

1.2.1 Burner Types

Burners are classified into five main categories which can be listed based on the type of mixing, fuel, operation, combustion air and burner body as given in **Table 1.2**. Burners are designed to achieve usage of different types of fuels efficiently in energy production and to have low emission rates according to system requirements and regulations. [6]

Table 1.2: Burner Types

Mixing	Fuel	Operation Type	Combustion Air	Burner Body
Premix	Gas Fuel	One Stage	Atmospheric	Monoblock
Partially Premix	Liquid Fuel	Multi Stage	Fan Asisted	Duoblock
Non-premix	Solid Fuel	Modulating		
	Dual Fuel			

The common classification method of burners is how the fuel and the oxidizer are mixed. Flame length, emission reduction, combustion safety are the main reasons for using different types of mixing styles.

Premixed burners, fuel and oxidizer mixed in a mixer before the combustion process begins. They have shorter flames compare to non-premixed burners. [1]

Partially premixed burners, some fraction of the fuel is mixed with the oxidizer. They are generally used for the safety reasons to reduce flashback risk. [1]

Non-premixed burners, fuel and oxidizer are separated and they mix before combustion process. They have longer flames and uniform temperature distribution compare to premixed burners. [1]

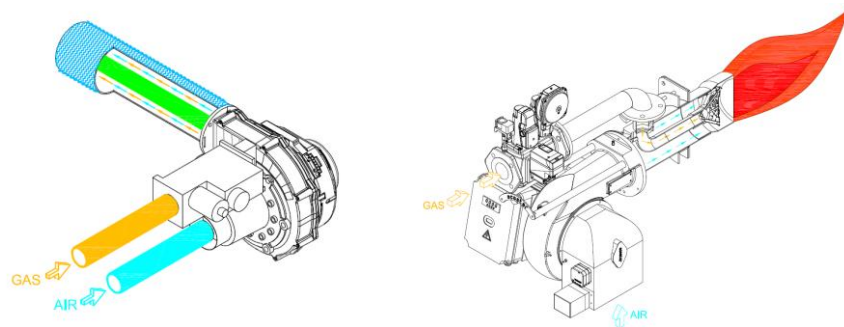


Figure 1.2: Premixed and Non-premixed burner

Operation type means how the burner load stage control is done. Manual or electronic fuel/oxidizer stage control is specified the burner operation type.

One stage burners operate in single-state load; fuel and combustion air delivery is constant. Burners can work on-off.

Multi stage burners can work in two stage or more load stages. Burners operate in both low load and high load points and a servomotor adjusts the fuel-air ratio in load stages.

Modulating burners operate in every point between low load and high load. Servomotors adjust the fuel-air ratio in every step.

Modulating burners are more efficient compared to one and multi stage burners. Start/stop of the burner during the operation cools the combustion chamber and causes energy losses. Modulating burners can work continuously during the energy production; continuously working principle provide energy saving. One stage and multistage burners have capacity limit due to safety regulations and design limits. [6]

Combustion air type is about how burner uses air to oxidize combustion reaction. Atmospheric and fan assisted burner types are specified.

In atmospheric burners, the air is fed to burner without any fan usage to oxidize combustion. They have limited capacity due to the air demand. Control of the atmospheric burner is more difficult compared to fan assisted burners. Atmospheric burners are used in slow changes of thermal output application such as chemical and hydrocarbon processing furnaces. Atmospheric burners combust generally gaseous fuels. [1]

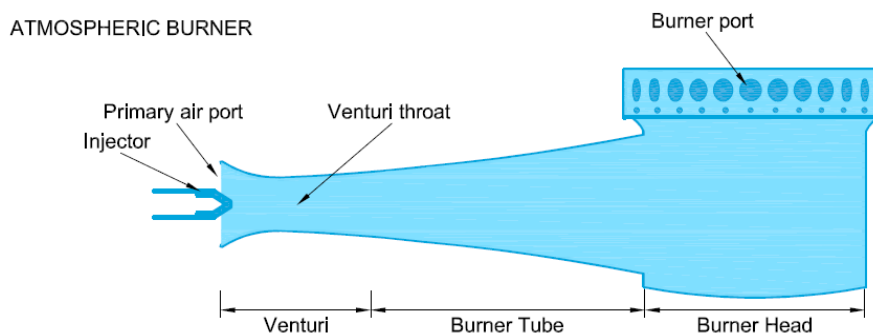


Figure 1.3: Atmospheric burner

Fan assisted burners have an internal or external air fan to supply oxidizer to the combustion reaction. Fan assisted burners have different control option such as one stage, two stage and modulation that provides high modulation for wide range of applications.

Fan integration is one of the most important design limit for the burner design. Fan capacity and pressure directly affect the burner performance.

Monoblock burners have body integrated fan and fan motor. They have limited capacity compared to duoblock burners due to fan design limits. Boiler back-pressure negatively affect burner capacity. Easy installation and operation are possible in monoblock burners due to the compact design.

Duoblock burners need combustion air fan integration with air ducts. They can work in higher capacity ranges compared to monoblock burner. External fan integration make possible to settle back-pressure negative affect instead of changing burner. External fans make possible duoblock burners adapting to wide range of processes.

Monoblock burners are compact and they have advantages of easy installation and operation. Duoblock burners have advantages of the external fan integration which provides easy solutions for the conditions such as less oxygen content due to the altitude and boiler/furnace back pressure-capacity problems by using the same burner body.

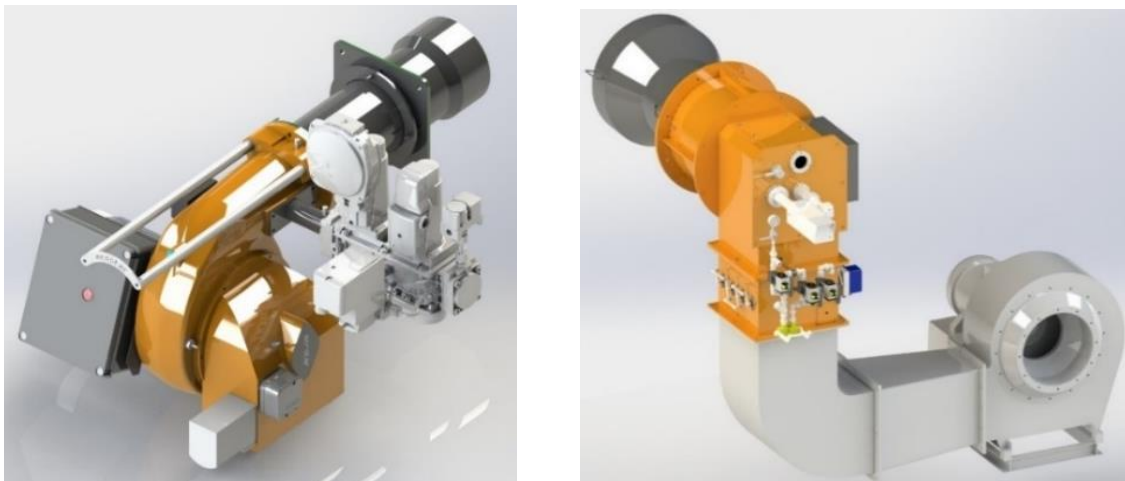
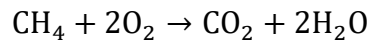


Figure 1.4: Monoblock and Duoblock Burner

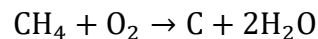
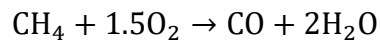
1.3 Combustion Stoichiometry and Combustion Products

A stoichiometric combustion mixture contains the exact amount of fuel and oxidizer. When the combustion is completed, all the fuel and oxidizer are consumed and form combustion products. This ideal mixture approximately yields the maximum flame temperature, and the energy released from combustion is used to heat the products. [7-9]

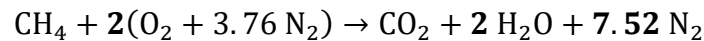
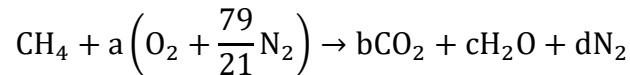
In complete combustion, oxidizer reacts with fuel and produces only carbon dioxide and water. For instance; the complete combustion reaction of methane is;



In incomplete combustion, oxidizer reacts with a hydrocarbon fuel and main combustion products are carbon dioxide, water, carbon and carbon monoxide. Due to carbon monoxide in products less energy is released than complete combustion and carbon monoxide is a poisonous gas. Incomplete combustion reaction of methane is;



The stoichiometric combustion reaction of methane where air consisting of 21% O₂ and 79% N₂ by volume is assumed as:



which shows per one volume of methane it requires two volumes of oxygen to complete its stoichiometric combustion.

Theoretical air requirement is the stoichiometric quantity of required amount of air for a complete combustion. From the stoichiometric combustion reaction of methane, 1 Nm³ methane required 9.52 Nm³ air to complete its combustion.

Equivalence ratio, is defined as the ratio of the actual fuel-air ratio to the stoichiometric fuel-air ratio. [1-2]

$$\Phi = \frac{(\text{Fuel}/\text{Air})_{\text{actual}}}{(\text{Fuel}/\text{Air})_{\text{stoichiometric}}} \quad (1.2)$$

$\Phi > 1$ is called rich mixture, $\Phi < 1$ is lean mixture and $\Phi = 1$ corresponds to stoichiometric mixture in fuel.

Excess air, is expressed as the percentage increase in the stoichiometric air requirement and it is defined by;

$$\text{Excess Air} = \frac{(\text{Air/Fuel})_{\text{actual}} - (\text{Air/Fuel})_{\text{stoichiometric}}}{(\text{Air/Fuel})_{\text{stoichiometric}}} \times 100 \quad (1.3)$$

Excess air always reduces efficiency of a combustion process since some of the heat produces in combustion is stored in excess air. Excess air-flue gas product's changes graph is shown in **Figure 1.5**. [1-4]

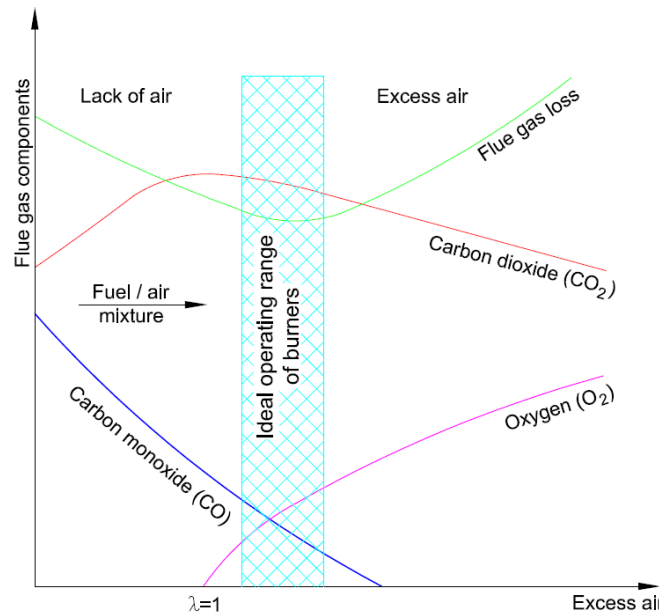


Figure 1.5: Excess air- flue gas products

Lambda (λ) is the ratio of the actual air-fuel ratio to the stoichiometric air-fuel ratio defined as;

$$\lambda = \frac{(\text{Air/Fuel})_{\text{actual}}}{(\text{Air/Fuel})_{\text{stoichiometric}}} = \frac{1}{\Phi} \quad (1.4)$$

If $\lambda > 1$ lean mixture in fuel, If $\lambda < 1$ rich mixture in fuel. Excess air decreases the flame temperature and combustion chamber temperature. To get the same load in excess air, there is need to burn more fuel. [1-4]

Lambda-flame temperature changes of natural gas graph is shown in **Figure 1.6**. [8]

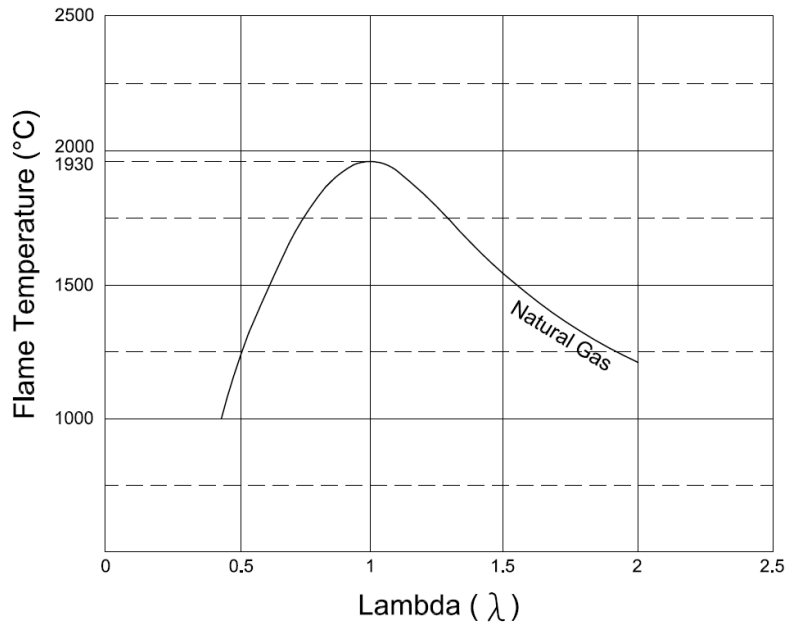


Figure 1.6: Lambda- flame temperature

1.4 Combustion Products

In combustion of hydrocarbon fuels, the products of combustion are distinctly identified as a source of environmental damage. The main combustion products are carbon dioxide, hydrogen oxide, carbon monoxide, nitric oxide and sulfur oxide (in case of solid fuels). Main pollutants are nitric oxide and sulfur oxide but recently even carbon dioxide considered harmful and have a significant effect on atmosphere and concerns rising in global greenhouse effect.

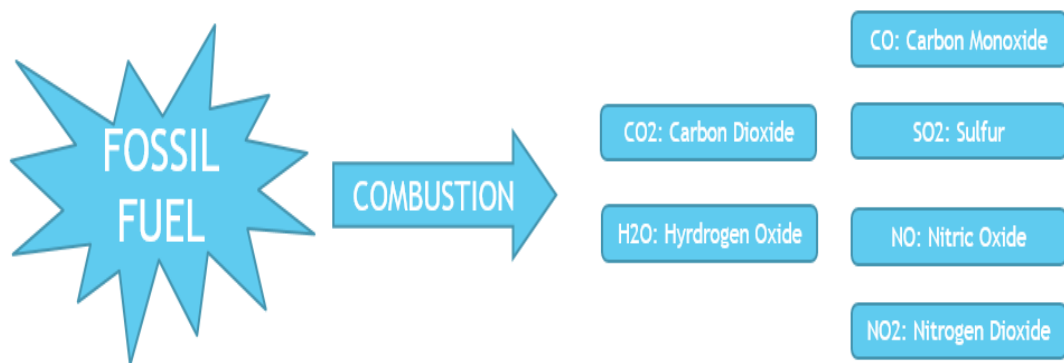


Figure 1.7: Fossil Fuel Combustion and Combustion Products

Main products of gas combustion are being explained in the following sections.

1.4.1 Carbon Dioxide

Carbon dioxide (CO_2) is one of the main products of hydrocarbon combustion. Higher the percentage of carbon dioxide in combustion product means higher energy output of combustion process. Lower CO_2 level causes higher fuel consumption due to the inefficient combustion and it increases the energy production costs.

Depending on the different hydrocarbon ratios in the fuels, the CO_2 levels vary. Common CO_2 values for different fuels are shown in **Table 1.3. [6,8]**

Table 1.3: Common emission values for a fan assisted burners

Fuel	Unit	O₂	CO₂
Natural Gas	%	3-4	9.8-11
Light Oil	%	3-5	12-14
Heavy Oil	%	3-5	11.8-13
Solid Fuel	%	5-6	12-14

1.4.2 Oxygen

Oxygen (O_2) availability in flue gas emission means excess air is supplied to the combustion process to be ensured to complete combustion. Higher oxygen concentration causes to reduction in efficiency, on the other hand lower oxygen concentration may cause incomplete combustion.

Depending on the different hydrocarbon ratios in the fuels, the O_2 levels may vary. Common O_2 values for different fuels are also shown in **Table 1.3. [6,8]**

1.4.3 Carbon Monoxide

Carbon monoxide (CO) is the indicator of the incomplete combustion and it is colorless, odorless, and tasteless gas. It has nearly the same density as air and it can easily mix into the air.

CO limits for liquid fuels combustion 110 mg/kWh, for gas fuel combustion 100 mg/kWh. **[11-12]**

1.4.4 Nitric Oxides (NO_x)

Most of the NO_x emissions consists of nitric oxide (NO) and contains nitric dioxide (NO₂) and nitrous oxide (N₂O). In the last half of the 20th century, NO and NO₂ are the major contributors to photochemical smog and ozone. NO_x participates in a chain reaction by removing ozone from the stratosphere, which allows increased ultraviolet radiation to reach the Earth's surface. NO_x is undesired pollutant combustion product and it is produced by the following three main route;

- Thermal NO_x
- Prompt NO_x
- Fuel NO_x

Effect of the lambda on combustion products is shown in **Figure 1.8. [10]**

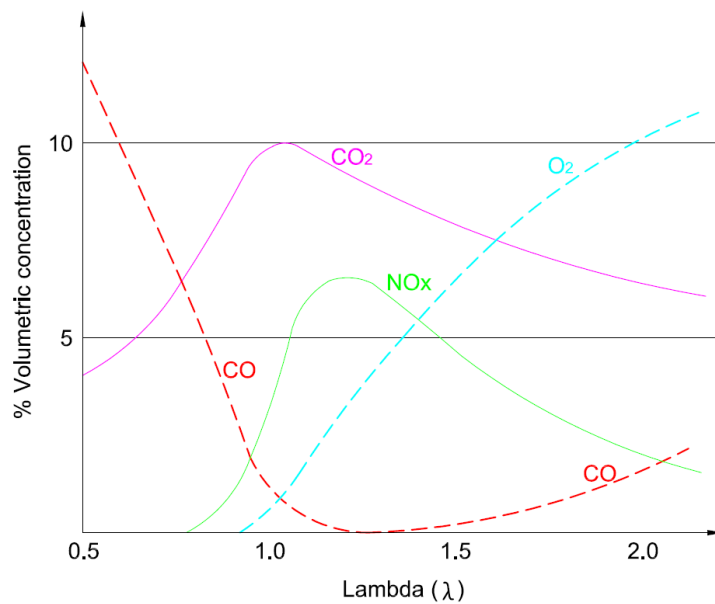


Figure 1.8: Combustion products (%) – Lambda

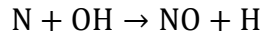
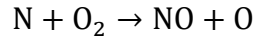
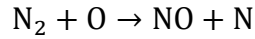
1.4.4.1 NO_x Mechanisms

NO_x formation mechanisms are explained in detail in this section.

Thermal NO Mechanism that is well known as **Zeldovich Mechanism** is the largest contributor to NO_x emissions and formed by oxidation of atmospheric nitrogen contained in combustion air at high temperatures. Flame temperature directly affects the thermal NO_x emissions, under high temperature conditions; $T > 1500\text{K}$, nitrogen in

combustion air is oxidized. Enriched oxygen combustion and preheated combustion air temperature directly affect flame temperature and thermal NO formation. [1,2,13]

Zeldovich Mechanism is;



The Prompt Mechanism is fast reaction between hydrocarbon and nitrogen in combustion air to form hydrocyanic acid (HCN) and known as Fenimore Mechanism. Hydrocyanic acid reacts with nitrogen and oxygen in combustion air and forms NO_x. Prompt mechanism reactions are very complicated and consist of hundreds of reactions. [1,2,13]

Prompt NO_x is an important factor of NO_x formation in low temperature and under stoichiometric combustion. Prompt NO_x is the small portion of the total NO_x emissions and its control is important to reach single digit NO_x emission values. Prompt-Fenimore's NO_x formation reactions are shown in **Figure 1.9**. [1,13]

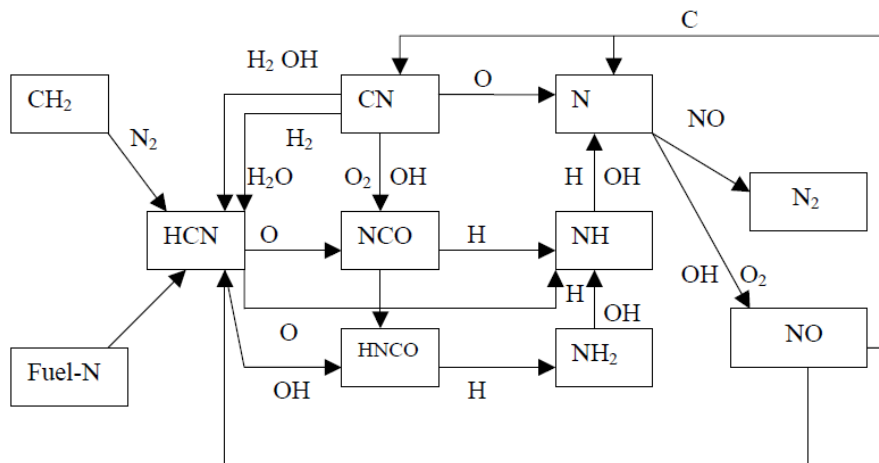


Figure 1.9: Prompt-Fenimore NO_x formation

Fuel NO_x is formed by oxidation of nitrogen in fuel and oxygen in the air. Gaseous fuels such as natural gas, propane are no bound nitrogen fuels. During the combustion of the liquid fuels and solid fuels that are consisted of fuel-bound nitrogen, 20%-50% of NO_x is formed due to the fuel NO_x. Fuel NO_x is generally important in non-premixed

combustion, in premixed combustion, fuels that are used in non-premixed combustion is generally gaseous fuels that contain little amount of nitrogen or no bound nitrogen.

Fuel NO_x formation reactions shown in **Figure 1.10**. [1]

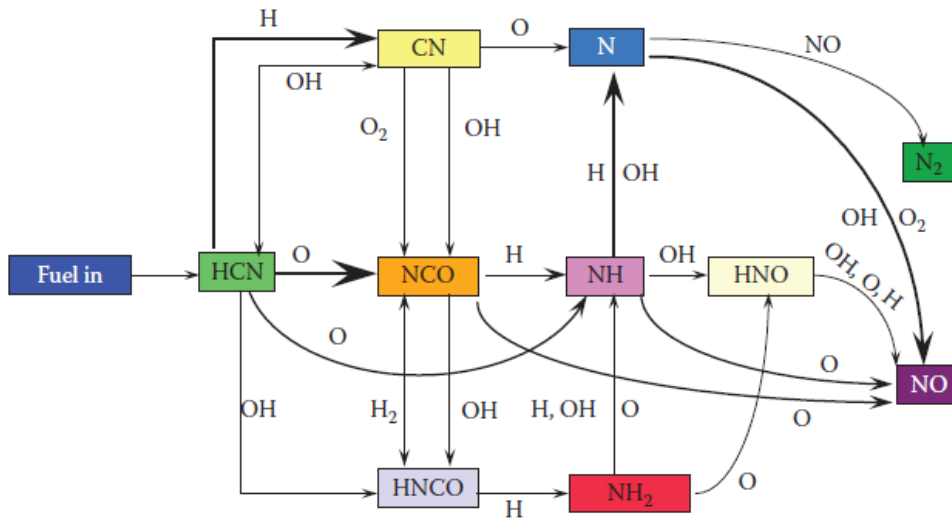


Figure 1.10: Fuel NO_x formation

Flame temperature primarily affects thermal NO_x and nitrogen content of the fuel affect fuel NO_x formation. NO_x reduction techniques are classified in two groups; combustion control techniques and post combustion control method. Post combustion control methods are more expensive compared to combustion control technique and they are not cost effective for loads lower than 30 MW. NO_x reduction methods for combustion control technique will be explained in detail in the next section.

1.4.4.2 NO_x Reduction Techniques

NO_x reduction is achieved by modifying the combustion process. Among common methods for modifying combustion process are external flue gas recirculation (EFGR), internal flue gas recirculation (IFGR), stage combustion and premixed combustion. [1,6] NO_x reduction techniques will be discussed in the next parts.

External flue gas recirculation (EFGR) is a method to reduce NO_x emission by recirculating flue gases from exhaust to burner. EFGR requires a fan, circulation pipes, adjustable air damper and special burner design to adapt gas recirculation inlet.

A portion of flue gases is recirculated back into combustion zone and recirculated hot flue gases which are cooler than the flame reduces flame temperature. This technique results in decrease in peak flame temperature and provides uniform flame temperature that causes reduction in NO_x emissions. Schematic working principle of EFGR is shown in **Figure 1.11**. [1,6]

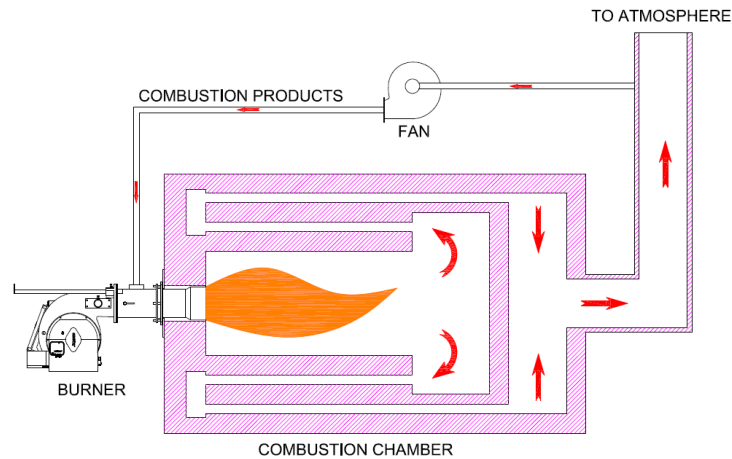


Figure 1.11: External flue gas recirculation

Internal flue gas recirculation (IFGR), is a method to reduce NO_x emission by recirculating flue gases inside the combustion chamber in combustion zone. IFGR does not require any special devices for recirculation, it is achieved by burner design that makes flue gas recirculation possible inside the combustion chamber. Flue gases are recirculated back into flame and the recirculated hot flue gases, cooler than flame, reduce flame temperature similarly as in EFGR. Schematic of the working principle of internal flue gas recirculation is shown in **Figure 1.12**. [1,6]

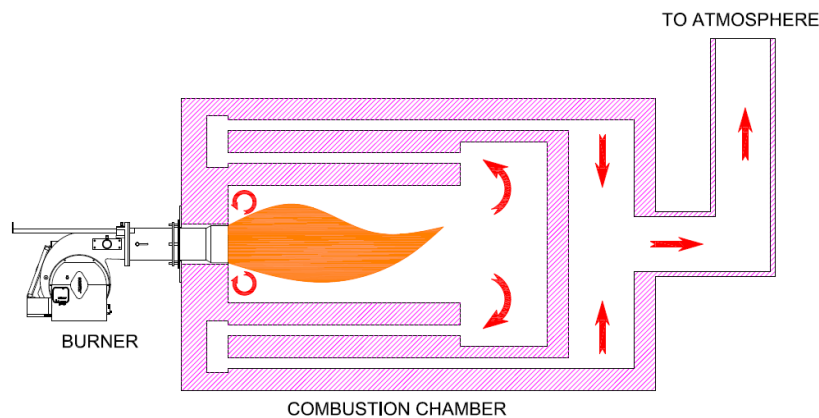


Figure 1.12: Internal flue gas recirculation

Stage combustion is classified into two techniques; staged air combustion and staged fuel combustion. For **air-staged combustion**, combustion air is divided into different streams. In the first stream, air is mixed with fuel corresponds to $\lambda < 1$ rich mixture in fuel. Unburned combustibles in the first stream of the flame are combusted by the second and tertiary streams. Overall combustion stoichiometry is nearly same at the end of the combustion process same as the conventional burner. Lower flame temperatures help to reduce NO_x emissions. [1]

For **fuel-staged combustion**, combustion air is divided into different streams as in air staged combustion. In the first stream, air is mixed with fuel $\lambda > 1$ corresponds to very lean mixture in fuel. Excess air from the first stream is used to combust fuel in the second and tertiary streams. Overall combustion stoichiometry is nearly same at the end of the combustion process as in the conventional burner. Lower flame temperatures help to reduce NO_x emissions. Schematic working principle of air staged combustion and fuel staged combustion are shown in **Figure 1.13**.

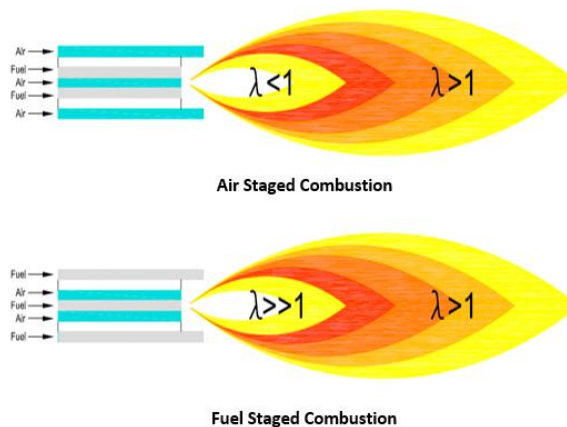


Figure 1.13: Stage combustion

Premixed combustion is restricted in higher loads (Load < 3-4 MW) due to the material thermal properties, design limits and high product costs. Schematic working principle of premixed combustion is shown in **Figure 1.14**.

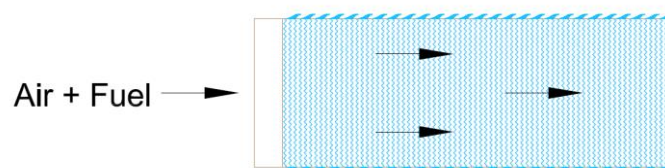


Figure 1.14: Premixed combustion

1.4.4.3 CO and NO_x Limits and Regulations

The NO_x limitations are varied depending on the application and application capacity. EN 676:2008, Automatic forced draught burners for gaseous fuels standard's emission classes are shown in **Table 1.4** with CO reference <100 mg/kWh. [11]

Table 1.4: EN 676:2008 NO_x Limitations-Emission Class

CLASS	mg/kWh	mg/m ³	ppm
1	170	169.59	82.56
2	120	119.71	58.28
3	80	79.1	38.85

Conversion of the NO_x (as NO₂) and CO emission values for natural gas are shown in **Table 1.5**. [14]

Table 1.5: Conversion of the NO_x and CO emissions for natural gas

			G20		G25	
			mg/kWh	mg/MJ	mg/kWh	mg/MJ
O ₂ =3%	NO	1 ppm	2.059	0.572	2.098	0.583
		1 mg/m ³	1.002	0.278	1.021	0.284
	CO	1 ppm	1.253	0.348	1.278	0.355
		1 mg/m ³	1.002	0.278	1.021	0.284

1.5 Literature Review

Literature review is done for both experimental and numerical studies that are related to burner design, burner optimization, combustion of different types of fuel and combustion in different applications. In this section of the thesis study, numerical and/or experimental studies found in literature are presented.

Šarlej et al. [15] focused on application of computational fluid dynamics (CFD) in an experimental low-NO_x burner design for a two-stage natural gas burner with a capacity of 0.5 MW to 1 MW. Mesh studies were done in GAMBIT and CFD studies were performed in ANSYS-FLUENT. A set of 27 geometric alternatives were introduced to identify an optimum geometry of the secondary fuel nozzles of an experimental burner

in terms of minimum NO_x production. Simplified geometries were used in CFD studies. Air duct was not modelled, simplification in swirl generator made the geometry symmetrical. With a symmetry in geometry one-fourth of the geometry was modelled and mesh element number was reduced. Water cooling section was modelled with a constant wall temperature boundary condition.

Turbulent flow was modelled by using $k-\omega$ turbulent model and chemical reactions were modelled by two-step simple methane combustion. Rates of chemical reactions were modelled by Eddy-dissipation model and radiative heat transfer was modelled by the discrete ordinates model. Mass flow inlet was used for the both fuel and air inlet as a boundary condition. Constant wall temperature was defined for the outer shells of the furnace and pressure outlet boundary condition was defined. An alternative corresponding to minimum NO_x production was identified and compared to an alternative with highest concentration of NO_x .

Chacon et al. [16] discussed a new methodology for the design and optimization of a 2 MW low NO_x monoblock natural gas burner that are studied in a superheated steam boiler. They were completed their studies experimentally and numerically. Numerical studies were done by using ANSYS-FLUENT software. Numerical model validated with experimental prototype. Same burner geometry was used for the different air/fuel ratios. Hexahedral meshes were used for the CFD model which had 350000 cells.

Turbulent flow was modelled by using $k-\varepsilon$ turbulent model. Flamelet combustion model and P-1 radiation model were used during the numerical studies. Mass flow inlet was used for the both fuel and calculated mass flow air inlet. Constant wall temperature was defined for the outer shells of the boiler. Pressure outlet boundary condition was defined. One of the best geometry was chosen and tested as a prototype burner.

Oystein Spangelo [17], investigated the influence of changes in the burner geometry on the emissions of NO_x and fuel supply pressure for a swirl burner. He has performed experimental, theoretical and numerical studies. 2D computational model of 20 kW burner were used. Tests are performed with 20 kW burner in an uncooled and a water-cooled combustion chamber.

Turbulent flow was modelled by using $k-\varepsilon$ turbulent model. Eddy Dissipation model, the Equilibrium PDF model and Flamelet PDF model were used for combustion

modeling. Flamelet PDF model were found to be most suitable model for combustion modelling. %3 O₂ referenced corrected NO_x emissions values have been measured 25 and 45 ppmv for methane and propane as fuel respectively for patented burner concept. Internal gas recirculation, rapid air and fuel mixing were used for NO_x reduction. Optimized burner was scaled successfully to 200 kW and 370 kW by using constant velocity scaling criteria which is commonly used for industrial burners.

Saripalli [18] discussed combustion and thermal flow behaviors for an industrial steam boiler application to identify how to increase boiler efficiency and how to reduce flue gas emissions. Methane was used as fuel. 3D computational geometry was modelled and meshed in GAMBIT and model was imported to CFD solver software ANSYS-Fluent for the numerical studies. Numerical model consists of four sections such as burner, combustion chamber, saturating part and superheating part.

Turbulent flow was modelled by using k-ε turbulent model. Mass flow inlet was used for the both fuel and air as a boundary condition. Constant wall temperature was defined for the outer shells of the boiler. Pressure outlet boundary condition was defined. Radiation was modelled by using the Rosseland radiation model. Combustion of methane was modelled by a single step reaction of finite-rate chemistry model. The overall simulation was provided comprehensive information about the modelled industrial steam boiler. Several ideas were formed to improve boiler efficiency and minimizing thermal stresses.

Khanafer et al. [19] investigated effect of swirl velocity and burner wall temperature on NO_x formation for an industrial swirl burner. Numerical studies were done by using commercial software FIDAP that uses finite element method. 2D axisymmetric geometry was used. The main goal of this study was to understand impact of design parameters on NO_x formation for gas fueled swirl burner. 85% methane and 15% nitrogen fuel composition were used and air used as an oxidizer for the simulations.

Turbulent flow was modelled by using k-ε turbulent model. Mass flow inlet was used for the both fuel and air as a boundary condition. Constant wall temperature was defined for the outer shells of the boiler. Combustion reaction was modelled with 2-step methane combustion. It was found that swirl enhances the mixing of air-fuel streams and leading to reduce flue gas emissions. Study showed that CO and unburned

hydrocarbons can be reduced about 3-5 times depending on swirl velocity. It was seen that the concentration of NO_x at the outlet do not decrease with swirl.

Kadar [20] discussed turbulent non-premixed combustion in rotary kiln industrial furnace to reduce NO_x formation due to stringent global NO_x emission standards. Free and open source CFD software OpenFOAM and Fluent were used in numerical solution and comparison were done for the results of the both software. For comparison of cold flow studies showed nearly identical results. For the reactive studies, temperature distribution; far from the inlet is in very good agreement but there were differences close to the inlet. Mass fractions for different species along the furnace axes showed good agreement.

2. MATERIAL and METHOD

In this thesis study, the combustion of natural gas has been examined using both numerical and experimental methods. A sample burner was chosen and then modelled using Fluent software. Fluent is a well-known commercial program used in both academic and industrial modeling studies. Two types of combustion chamber geometries and three burner geometry have been studied. Numerical results have been validated with available experimental data.

2.1 Experimental Setup

In order to measure the temperature levels at different locations of the combustion chamber and the flue gas emissions, the experimental setup located in ECOSTAR company is utilized. Test setup, measurement devices, burner and combustion chambers technical specifications are being explained in the following parts of this chapter.

2.1.1 Test Setup

Burner tests are conducted in ECOSTAR Combustion Systems R&D laboratory with a wide range of operating parameters. R&D laboratory has test capacity between 20 kW to 5 MW. Measurements can be performed with different types of fuels such as natural gas, light oil, heavy oil, waste oil and LPG.



Figure 2.1: ECOSTAR R&D Laboratory

The following operating parameters are being measured during the tests in line with PLC controlled test units;

- Fuel flow rate,
- Fuel supply temperature and pressure,
- Cooling water flow rate,
- Cooling water inlet and outlet temperature,
- Flue gas emissions (CO, CO₂, O₂, NO_x, SO_x)
- Flue gas temperature,
- Boiler back pressure,
- Fuel and combustion air pressure,

Thermal imaging can be done with two thermal cameras as well.

2.1.2 Combustion Chamber Technical Specifications

Two different combustion chambers were used during the experimental studies. First combustion chamber (**FCC**) is a hot water test boiler that has a capacity of 1000000 kcal/h and has a movable rear wall to adjust combustion chamber length. Second combustion chamber (**SCC**) is direct fired and non-cooled. Electronically controlled flue gas damper enables adjusting boiler back-pressure for the both combustion chambers. Dimensions of the combustion chambers are shown in **Figure 2.2**.

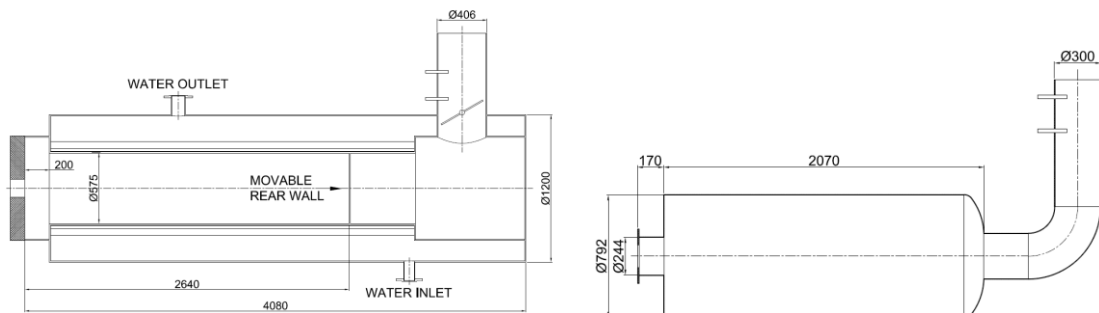


Figure 2.2: Dimensions of the FCC and SCC

In **Figure 2.3** the schematic of test setup is given.

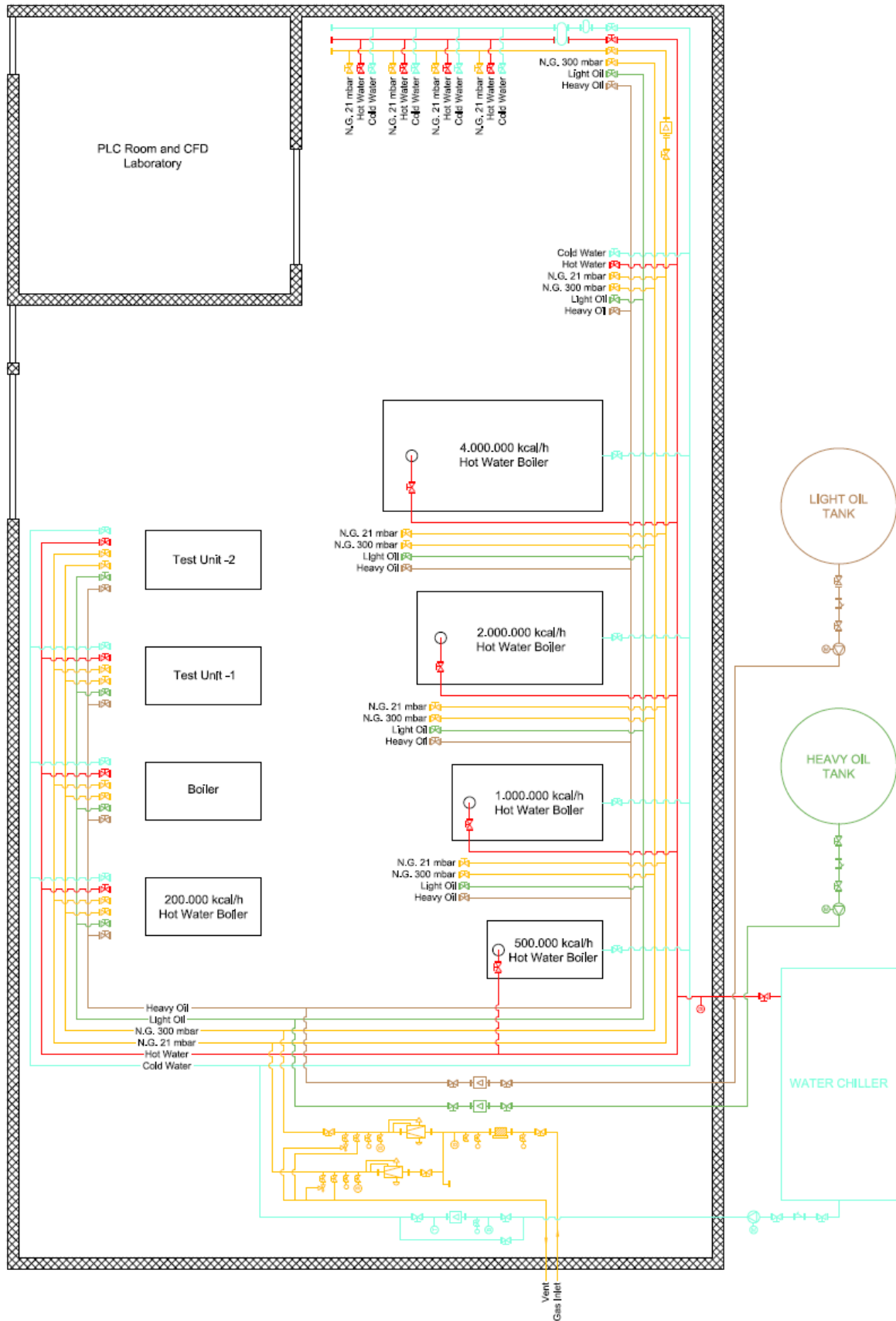


Figure 2.3: Flow Diagram of the ECOSTAR R&D Laboratory

2.1.3 Measurement Devices

Available measurement devices and their technical specifications such as measuring parameters, measuring range and accuracy are listed below in **Table 2.1**.

Table 2.1: Measurement Devices

No	Device	Brand	Parameter	Range	Accuracy
1	Gas Analyzer	MRU-Nova Plus	O ₂	0-21%	±0.2%
			CO	0-4000 ppm	±10ppm
			CO ₂	0-30 %	±0.3
			NO	0-1000 ppm	±5 ppm
			NO ₂	0-200 ppm	±5 ppm
			SO ₂	0-2000 ppm	±10 ppm
			°C	0-650°C	±2°C
2	Gas Analyzer	MRU Optima-7	O ₂	0-21%	±0,2%
			CO	0-4000 ppm	±10ppm
			CO ₂	0-30 %	±0.3
			NO	0-1000 ppm	±5 ppm
			NO ₂	0-200 ppm	±5 ppm
			SO ₂	0-2000 ppm	±10 ppm
			°C	0-650°C	±2°C
3	Gas Analyzer	ABB EL 3020	O ₂	0-25 ppm	
			CO	0-3000 ppm	
			CO ₂	0-20 %	
			NO	0-1000 ppm	
			SO ₂	0-3000 ppm	
4	Pressure Transmitter	ABB 2600 T	P		
5	Temperature Transmitter	ABB TSP 121	T	-40 400°C	±0.3±0,005T
6	Thermal Mass Flowmeter	ABB FMT500-IG	Nm ³ /h	0-1300	<0.1*M.V.
7	Electromagnetic Flowmeter	ABB FEP300	m ³ /h		
8	Gas Leak Dedector	Testo-316-1	CH ₄	0-10000 ppm	
9	Thermal Imager	TESTO-881	°C	0-350°C	±2°C
10	Thermal Imager	Optirus	°C/K	-20 °C 900 °C	
11	Sound Level Meter	Testo-816	dB	30-130 dB	±1dB
12	Multichannel Thermometer	Testo-735-2	T	-200 to +1000 °C	0.2 °C + 0.3% of M.V.
13	Pressure Measuring Inst.	DM 9200	mbar	0-350	
14	Pressure Measuring Inst.	DM 9200	mbar	0-1000	
15	Pressure Measuring Inst.	TESTO 312-3	mbar	-300 to 300	±0.1*M.V.
16	Anomometer	Testo 410-1	m/sn	0,4-20 m/sn	±0.2 m/sn
17	Anomometer	Testo 435	m/sn	+0.6 +40 m/sn	±0.2 m/sn
18	Anomometer	Testo Hygrotest	m/sn		

2.1.4 Burner Technical Specifications

In this study, ECOSTAR ECO-45 G C burner is considered. It is a non-premixed type, monoblock modulating and natural gas/LPG burner. General specifications of ECO-45 G C burner is listed in **Table 2.2**.

Table 2.2: Burner General Specifications

Fuel Type	Natural Gas-LPG	Ignition	Direct Ignition
Operating Type	Modulating	Flame Control	Ionization

Four different capacities, given in **Table 2.3**, can be obtained using the same burner body. Capacity changes are provided by fan design, fan motor power and gas adjusting valve. Technical specifications are listed in **Table 2.3**.

Table 2.3: Burner Technical Specifications

BURNER TYPE	CAPACITY		CAPACITY		NATURAL GAS CONSUMPTION		FAN MOTOR POWER	MAIN SUPPLY
	Min. kcal/h	Max. kcal/h	Min. kW	Max. kW	Min. Nm ³ /h	Max. Nm ³ /h	kW	VAC
ECO 45 G C 2	172,000	645,000	200	750	20.8	78.2	0.75	3N 380
ECO 45 G C 2/L	172,000	749,920	200	872	20.8	90.9	0.75	3N 380
ECO 45 G C 2a	172,000	860,000	200	1,000	20.8	104.2	1.1	3N 380
ECO 45 G C 2b	172,000	1,032,000	200	1,200	20.8	125.1	1.5	3N 380

ECOSTAR ECO-45 G C gas burner has movable inner and fixed outer diffuser. Movable flame tube extension and movable inner diffuser enables adjusting desired CO, CO₂ and O₂, emission values in different combustion chamber designs.

Main burner equipment of ECO-45 are shown in **Figure 2.4**.

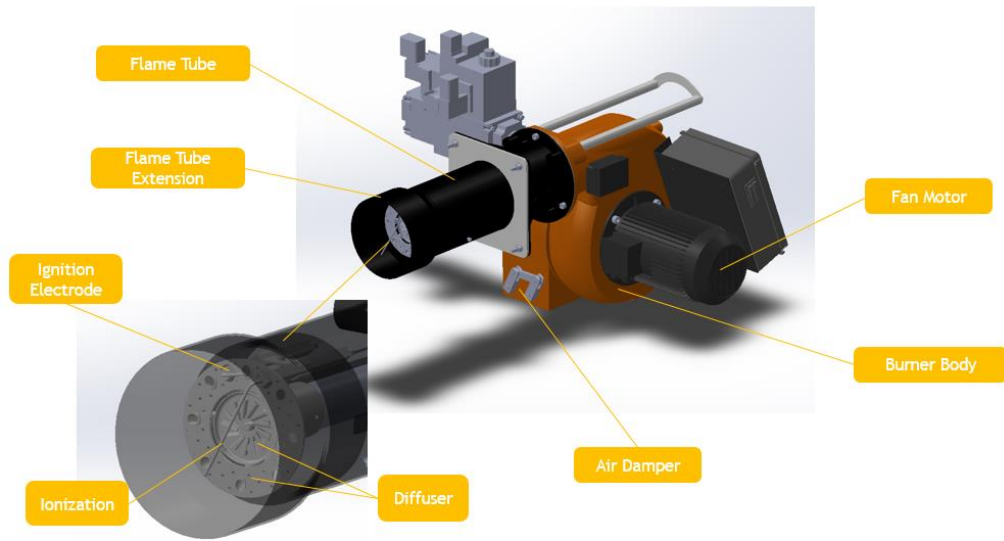


Figure 2.4: ECO-45 Gas Burner Equipment's

2.1.5 Fuel Composition

Fuel composition values of natural gas that was used during the experiments are taken from ÇORDAŞ- Tekirdağ Gas Company between 1st January 2016 and 19th January 2016. Average values are used during the numerical studies. 96.003% of the fuel composition is consisted of methane and percentage of other components are shown in **Figure 2.5**.

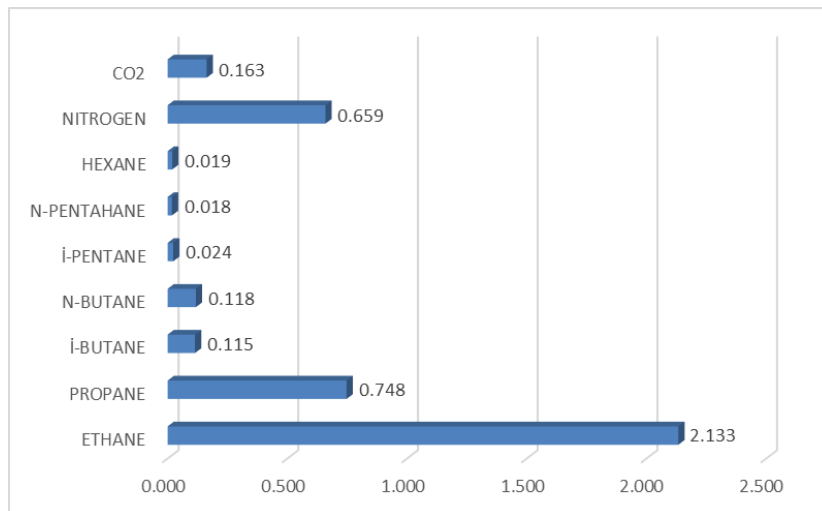


Figure 2.5: Fuel Composition (%)

Methane, ethane, propane and butane components are only considered in the numerical studies.

2.2 Numerical Methods

Numerical methods are cost effective and time saving tools for the new design, design optimization, product development and troubleshooting for engineering problems. There are various numerical solution techniques used for modelling which are finite difference, finite volume and finite element methods. Well-established CFD codes are used finite volume method such as ANSYS-CFX, ANSYS-FLUENT, Star CCM.

Some of the application area examples that use CFD are;

Power plant: Internal combustion engines, burners and gas turbines,

Marine engineering: Off-shore structures' load analysis,

Turbomachinery: Flow inside rotating passages,

Aerodynamics of vehicles: Aircraft, car design,

Hydrodynamic of ships

Electrical and electronic engineering: Cooling of equipment,

Environmental engineering: Pollutants and effluents distribution

Architecture and civil engineering: Wind loading and HVAC

In thesis study, ANSYS-Fluent software was used during the numerical studies. ANSYS-Fluent uses finite volume method for calculation of momentum, energy conversation, transport equation of mass and species composition. Mainly CFD software's have three main stages; **pre-processor, solver and post-processor.**

Pre-processing is input of a flow problem and description of the computational domain. Accuracy of a CFD problem solution is directly related to the mesh cell number and mesh quality. Generally higher cell number meshes has finer quality and higher accuracy. Higher cell number needs better computer hardware and numerical solutions take longer time. Meshes should be optimized in order to make design time and computational cost less. Pre-processing stage involves;

- Definition of the geometry to describe computational domain,
- Mesh generation of the fluid volume,
- Modelling of physical and chemical phenomena,
- Definition of fluid properties,
- Identifying boundary conditions.

Solver is the second stage of CFD calculations Solver stage involves;

- Governing equations integration to computational domain,
- Conversion of the integral equations into a system of algebraic equations,
- Solution of the algebraic equations by an iterative method.

Post-processor is the final stage of the CFD problem solution data visualization. Post - processor stage involves;

- 2D and 3D surface plots,
- Line and shaded contour plots,
- Vector plots,
- Animation of the problem results,
- Comparison of the solutions. [21]

2.3 Governing Equations

CFD calculations are governed by fluid flow governing equations. The governing equations for mass, momentum and energy are; [21,30]

Mass conservation;

$$\frac{\partial \rho}{\partial t} + \nabla \cdot \rho \mathbf{U} = 0 \quad (2.1)$$

Momentum;

$$\frac{\partial \rho \mathbf{U}}{\partial t} + (\nabla \mathbf{U} \cdot \rho \mathbf{U}) = -\nabla p + \nabla \cdot \boldsymbol{\tau} + \rho \cdot \mathbf{g} \quad (2.2)$$

Energy;

$$\frac{\partial (\rho E)}{\partial t} + \nabla \cdot (\vec{v}(\rho E + p)) = \nabla \cdot \left(k_{eff} \nabla T - \sum_j h_j \vec{J}_j + (\vec{\tau}_{eff} \cdot \vec{v}) \right) + S_h \quad (2.3)$$

2.4 Combustion Models

Combustion is an important topic in industrial applications such as power generation, steel and glass melting furnaces, gas flares and aerospace engineering etc. Accurate combustion modelling is important to predict equipment efficiency and reducing the non-desired combustion products. Modelling combustion is possible by simulating combustion realistically. Combustion depends directly on mixing and chemistry. The

relative speed of chemical reaction is critical and Damköhler number is used to specify chemical reaction speed.

Damköhler number (Da) represents the ratio of the characteristic turbulent mixing time to the characteristic chemical reaction time. Damköhler number equation is;

$$Da = \frac{\text{Mixing Time Scale}}{\text{Chemical Time Scale}} \sim \frac{L/U}{\rho_{ad}/R_{slow}} \sim \frac{k/\epsilon}{\rho_{ad}/R_{slow}} \quad (2.4)$$

ρ_{ad} : Adiabatic flame density

R_{slow} : Slowest reaction rate at T_{ad} and stoichiometric concentrations

If $Da \gg 1$, chemical reaction rates are fast. Reactions are limited by turbulent mixing. Selection of turbulence model is important. Combustion in furnaces, boiler, gas turbines, gasifiers and incinerators are examples of fast chemistry.

If $Da \approx 1$, chemical reaction rates are slow. Reactions are limited by chemistry and turbulence interactions. Selection of reaction mechanism and turbulence-chemistry interactions are important. Reactions related with pollutant formation, chemical vapor deposition and air dissociation at hypersonic speed are examples of slow chemistry.

Combustion models and combustion phenomenology is shown in **Figure 2.6.** [22]

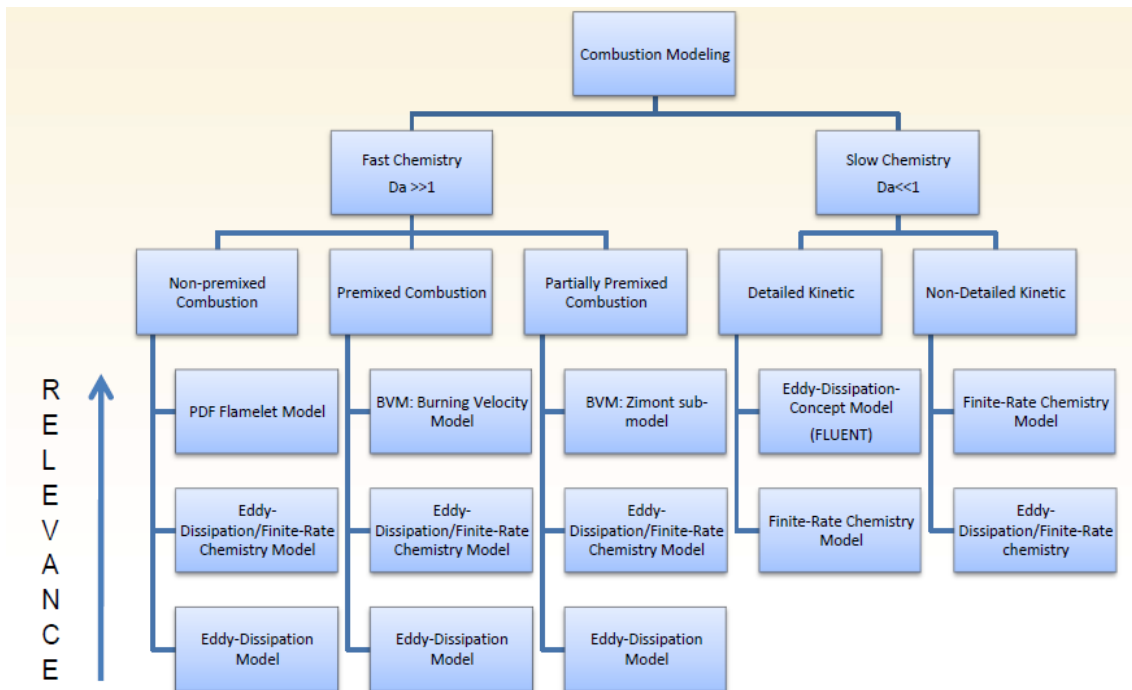


Figure 2.6: Combustion Phenomenology and Combustion Modelling

Combustion models that are used during numerical solutions are explained shortly below. [23]

Finite rate chemistry model ignores the effect of turbulent fluctuations and reaction rates are determined by Arrhenius kinetic expressions.

Eddy-Dissipation model is used one or two step heat release mechanisms for realistic results. Arrhenius chemical kinetic calculations can be avoided and Eddy-dissipation model is cost effective in combustion modelling.

Eddy-Dissipation/Finite-Rate model evaluates reaction rate by both model and the smallest one is chosen.

PDF Flamelet model is only applicable to a two-feed system; fuel and oxidizer. Mixture fraction and mixture fraction variance scalar quantities are solved besides the momentum and energy equations. Combustion species extracted from library as a function of mixture fraction and strain rate.

3. RESULTS and DISCUSSION

3.1 Experimental Studies

Experimental studies were performed in ECOSTAR R&D laboratory. Cooling water inlet-outlet temperature, flue gas emissions, fuel consumption and cooling water flow rate are measured and recorded by using PLC controlled measurement equipment's. Measurement points, measurement parameters and test setup for the first combustion chamber is shown in **Figure 3.1** and **Figure 3.2**; for the second combustions chamber in **Figure 3.3** and **Figure 3.4**



Figure 3.1: Test setup-1 (FCC)

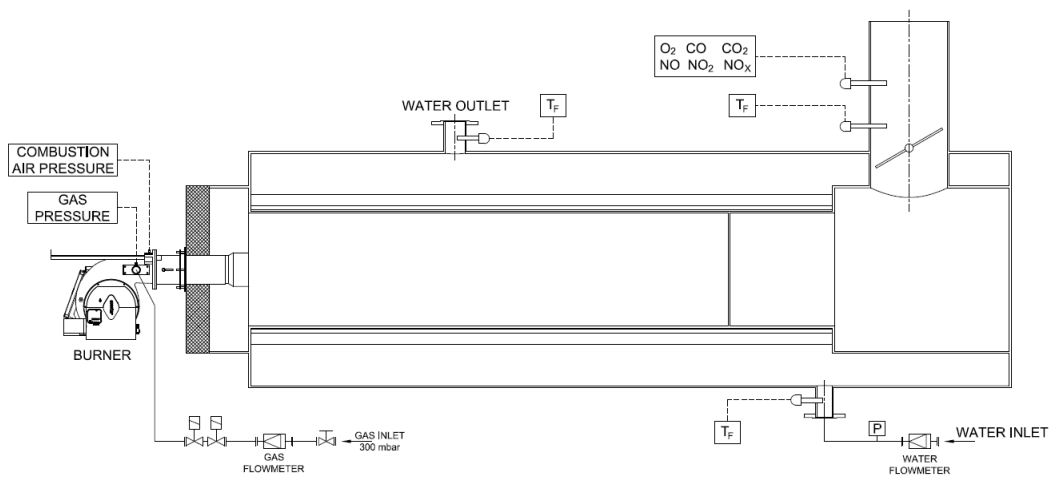


Figure 3.2: Test setup and measured operating parameters of the FCC



Figure 3.3: Test setup-2 (SCC)

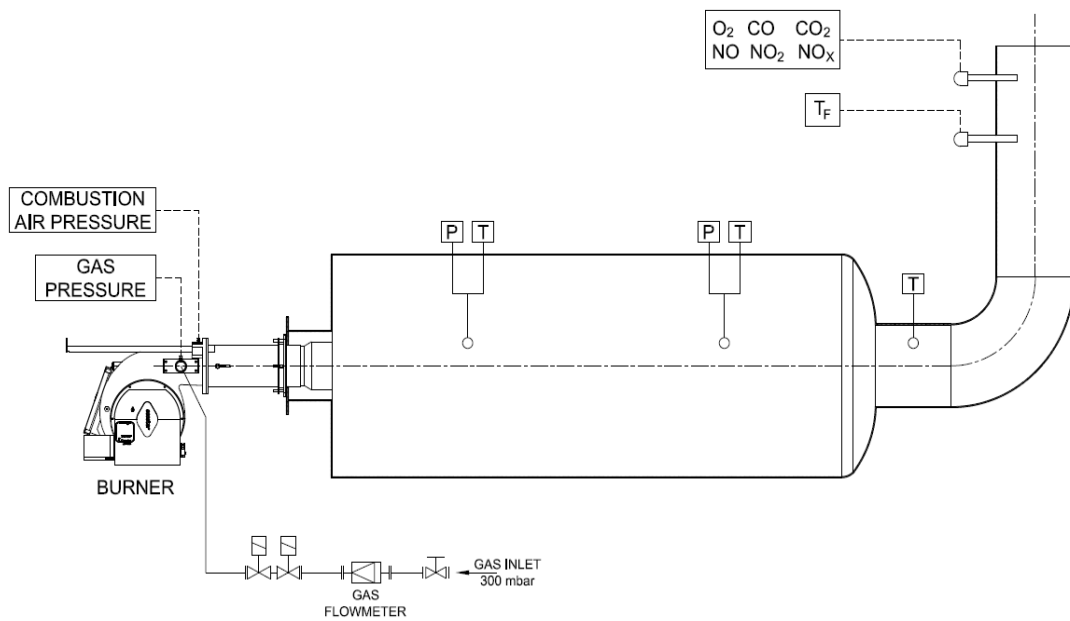


Figure 3.4: Test setup and measured operating parameters of the SCC

At first, experimental studies were done for the constant burner consumption in **high load** (125.1 Nm³/h) for the **different excess air** with standard ECO-45 burner geometry in **FCC**. Test conditions are listed in **Table 3.1**. Measured experimental values will be used in numerical studies later on.

Table 3.1: Test conditions for the experimental studies in FCC

Air Temperature	10	°C
Gas Temperature	13	°C
Gas Consumption	125.1	Nm ³ /h
Gas Inlet Pressure	300	mbar
Water Inlet Temperature	30	°C
Water Outlet Temperature	50	°C
Water Flow Rate	16.5	m ³ /h

Emission test results of first experiments are shown in **Table 3.2**.

Table 3.2: Emission test values for 125.1 Nm³/h gas consumption

Lambda		1.16	1.2	1.25	1.3	1.4
O₂	%	2.8	3.5	4.2	4.9	6
CO₂	%	9.84	9.76	9.14	8.77	8.18
CO	ppm	12	3	0	2	0
NO_x	ppm	68	63	60	57	51

Test results that are drawn by using the experimental measurements are shown in **Figure 3.5 - Figure 3.8**.

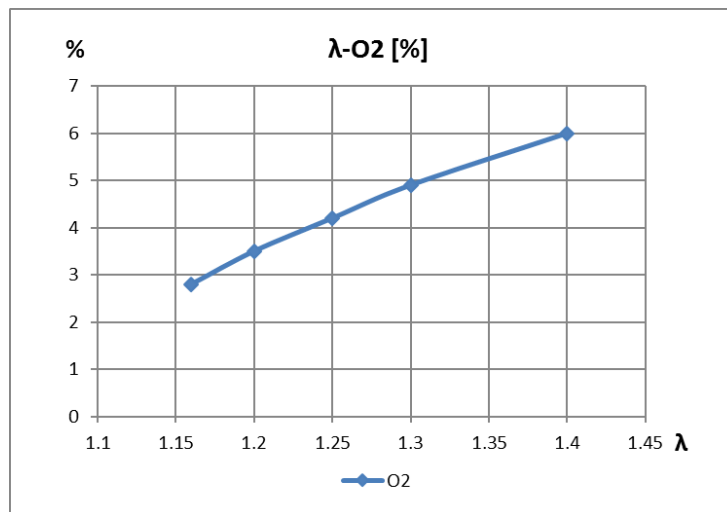


Figure 3.5: Lambda versus oxygen percentage [%]

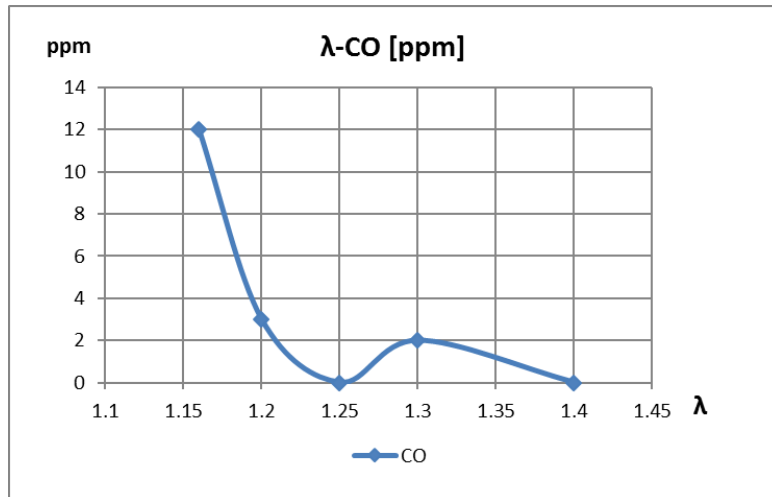


Figure 3.6: Lambda versus carbon monoxide [ppm]

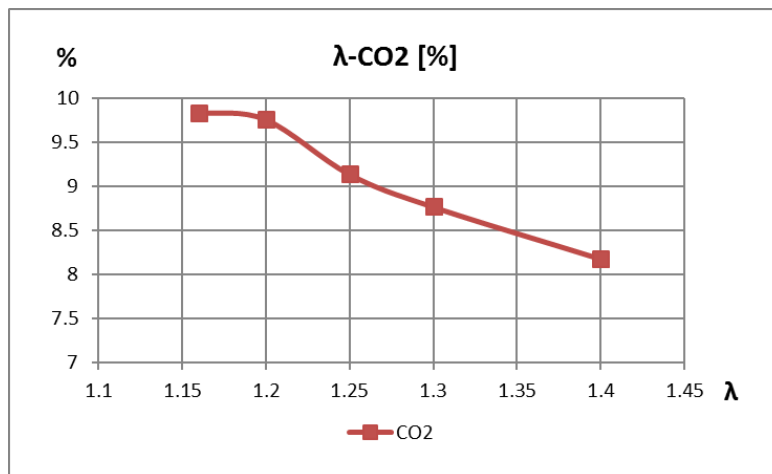


Figure 3.7: Lambda versus carbon dioxide percentage [%]

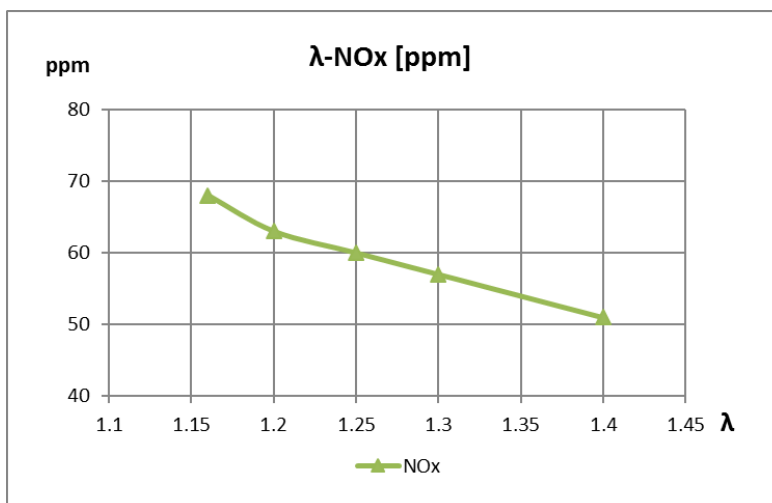


Figure 3.8: Lambda versus nitrogen oxide [ppm]

Secondly, experimental studies were done for the different burner **loads** for the $\lambda=1.2$ with standard ECO-45 burner geometry in **FCC**. Emission test results of second experiments are shown in **Table 3.3**.

Table 3.3: Emission test values for $\lambda=1.2$ in different burner loads

Fuel Type	Gas Consumption	λ	O ₂	CO ₂	NO _x
	Nm ³ /h	-	%	%	ppm
Mix Natural Gas	50	1.2	3.5	9.44	57
Mix Natural Gas	75	1.2	3.4	9.72	65
Mix Natural Gas	100	1.2	3.5	9.55	61
Mix Natural Gas	125.1	1.2	3.5	9.76	63

Test results that are drawn by using the experimental measurements are shown in **Figure 3.9 - Figure 3.11**.

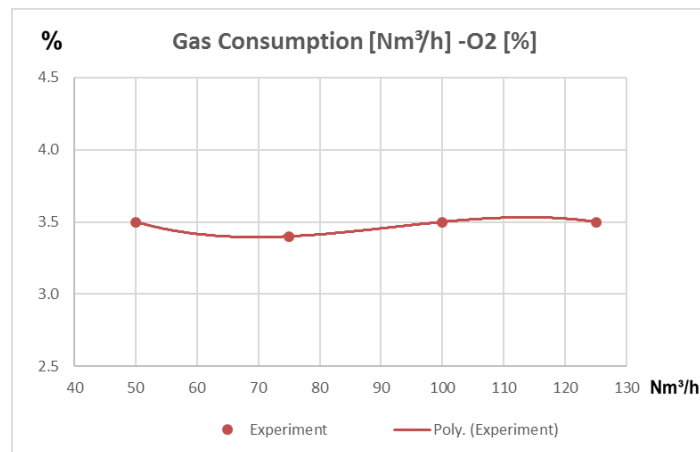


Figure 3.9: Gas consumption [Nm³/h] versus oxygen percentage [%]

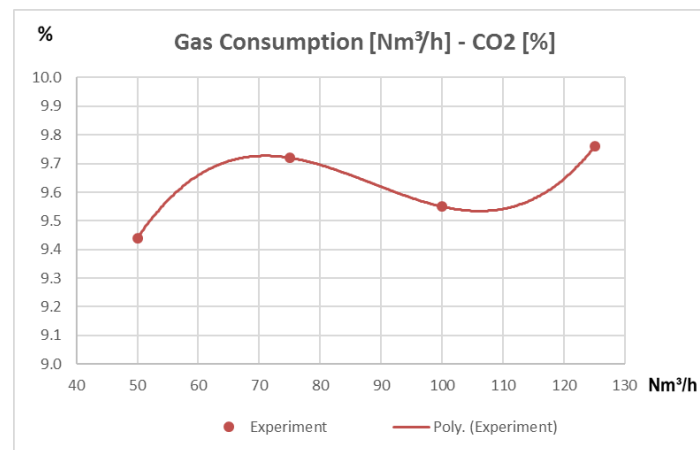


Figure 3.10: Gas consumption [Nm³/h] versus carbon dioxide percentage [%]

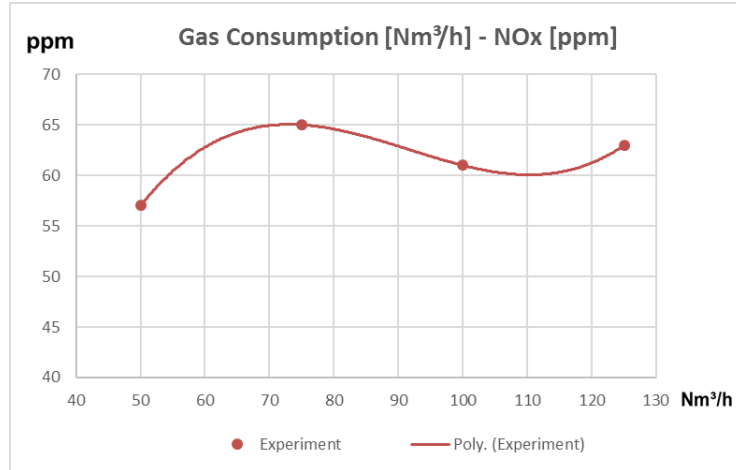


Figure 3.11: Gas consumption [Nm³/h] versus nitrogen oxide [ppm]

Thirdly, experimental studies were done for the constant burner consumption in **low-load** (35Nm³/h) for the ECO-45 burner geometry in **SCC**.

Experiments for the high load was not performed due to the higher temperatures. Test conditions and measured experimental values are listed in **Table 3.4**.

Table 3.4: Emission test values and test conditions of the second experiment

Fuel	Fuel Flow Rate	Gas Inlet Temperature	O₂	CO₂	NO_x
-	Nm ³ /h	°C	%	%	ppm
Mix Natural Gas	35	13	4.9	8.84	56

Thermal camera used for the wall temperature measurements and measured values is shown in **Figure 3.12** and **Figure 3.13**. Measured values are used during the numerical studies.

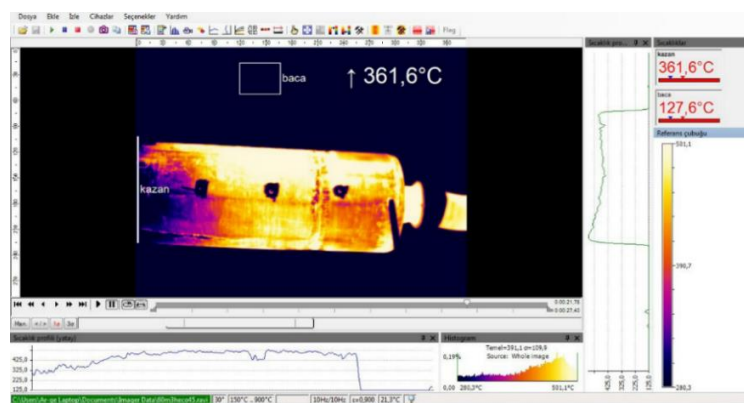


Figure 3.12: Thermal camera image of the combustion chamber during the experiments

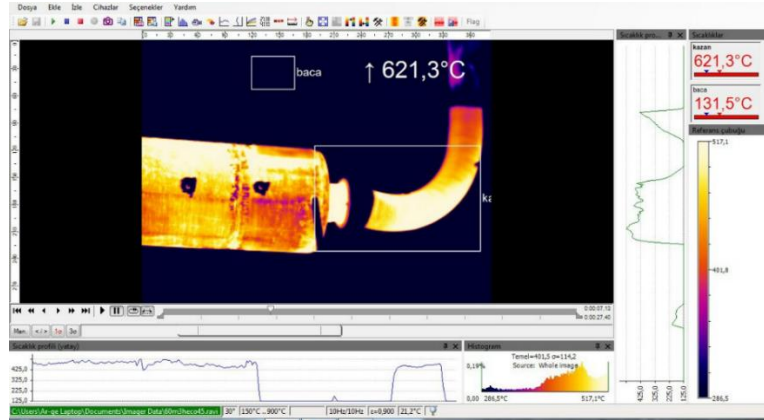


Figure 3.13: Thermal camera image of the flue part during the experiments

3.2 Numerical Studies

Numerical studies are performed using ANSYS-Fluent CFD solver. Geometries for the solutions are developed in Solidworks. Numerical studies are done in the following order;

1. Geometry is modelled in **Solidworks**,
2. Geometry is imported to **ANSYS Design Modeler** and fluid volume is created,
3. Created fluid volume is imported to **ANSYS Mesh** and then mesh is generated,
4. Generated mesh is imported to **ANSYS Fluent** solver. Cold flow and reactive analysis are done in Fluent by using calculated boundary conditions and experimental datas.

In the following part of the thesis study, calculated fuel-air ratios and calculations of the theoretical combustion products will be explained in detail.

3.2.1 Theoretical Air and Combustion Products Calculations

Theoretical air-fuel and combustion products are calculated by a developed MS-Excel code. Calculations are done for 100% methane in $\lambda = 1$ and $\lambda = 1.2$ and for mix natural gas in $\lambda = 1$ and $\lambda = 1.2$. Density calculations are done by using referenced website. Density calculations results are shown in **Table 3.5. [23]**

Natural gas density calculation is done for 100% methane and then calculated value is used for the theoretical air and combustion products calculations. Reference temperature

is chosen to be 15°C and reference pressure is 1.01325 bar. The calculated density of 100% methane is 0.68 kg/m³.

Table 3.5: Natural gas density calculation results for 100% Methane

Temperature	°C	15	Compression factor	-	0.998
Pressure	MPa	0.101325	Molar mass		16.043
Mass density	kg/m ³	0.68	Molar density		0.04238

Theoretical combustion equation and calculated wet and dry volumetric combustion products for $\lambda = 1$ are shown in **Table 3.6**.

Table 3.6: Theoretical combustion products calculations of 100% Methane, $\lambda = 1$

%100 CH4 Combustion Lambda=1						
1 CH4 + 2 (1 O2 + 3.8 N2) = 1 CO2 + 2 H2O + 7.52 N2						
Total Air Demand	9.52	m ³ /h				
Combustion Products						
	m ³ /h	Wet %	Dry %	Total Wet	10.520	m ³ /h
				Total Dry	8.520	m ³ /h
CO2	1	9.51	11.74			
H2O	2	19.01	-			
N2	7.52	71.48	88.26			

Total air demand is calculated for 1 m³ methane combustion. For $\lambda = 1$; 1 m³/h methane needs 9.52 m³/h air theoretically.

Theoretical combustion equation and calculated wet and dry volumetric combustion products for $\lambda = 1.2$ are shown in **Table 3.7**.

Table 3.7: Theoretical combustion products calculations of 100% Methane, $\lambda = 1.2$

%100 CH4 Combustion Lambda=1.2						
1 CH4 + 2 (1 O2 + 3.8 N2) = 1 CO2 + 2 H2O + 7.52 N2						
1 CH4 + 2.4 (1 O2 + 3.8 N2) = 1 CO2 + 2 H2O + 9.024 N2 + 0.4 O2						
Total Air Demand	11.424	m ³ /h				
Combustion Products						
	m ³ /h	Wet %	Dry %	Total Wet	12.424	m ³ /h
				Total Dry	10.424	m ³ /h
CO2	1	8.05	9.59325			
H2O	2	16.10	-			
N2	9.024	72.63	86.5695			
O2	0.4	3.22	3.8373			

Total air demand is calculated for 1 m³ methane combustion. For $\lambda = 1.2$; 1 m³/h methane needs 11.424 m³/h air theoretically.

Natural gas density calculation is done for natural gas mixture and then calculated value is used for the theoretical air and combustion products calculations. Natural gas composition that is used in theoretical calculations is shown in **Table 3.8**.

Table 3.8: Natural gas composition

Methane	%	96.064	Butane	%	0.233
Ethane	%	2.133	Nitrogen	%	0.659
Propane	%	0.748	Carbon dioxide	%	0.163

Reference temperature is 15°C and reference pressure is 1.01325 bar; calculated density of natural gas mixture is 0.711 kg/m³. Density calculations results are shown in **Table 3.9**. [23]

Table 3.9: Natural gas density calculation for natural gas mixture

Temperature	°C	15	Compression factor	-	0.9979
Pressure	MPa	0.101325	Molar mass		17.775
Mass density	kg/m ³	0.711	Molar density		0.0424

Theoretical combustion equation and calculated wet and dry volumetric combustion products for $\lambda = 1$ are shown in **Table 3.10**.

Table 3.10: Theoretical combustion products calculations of natural gas mixture, $\lambda = 1$

Mixed Natural Gas Combustion Lambda=1					
					Composition
1 CH ₄	+ 2 (1 O ₂ + 3.8 N ₂)	=	1 CO ₂	+ 2 H ₂ O + 7.52 N ₂	96.064
1 C ₂ H ₆	+ 3.5 (1 O ₂ + 3.8 N ₂)	=	2 CO ₂	+ 3 H ₂ O + 13.16 N ₂	2.133
1 C ₃ H ₈	+ 5 (1 O ₂ + 3.8 N ₂)	=	3 CO ₂	+ 4 H ₂ O + 18.8 N ₂	0.748
1 C ₄ H ₁₀	+ 6.5 (1 O ₂ + 3.8 N ₂)	=	4 CO ₂	+ 5 H ₂ O + 24.44 N ₂	0.233
Total Air Demand	9.75		m ³ /h		
Combustion Products		Wet	Dry	Total Wet	10.764
	m ³ /h	%	%	Total Dry	8.737
CO₂	1.04	9.62	11.8464		
H₂O	2.03	18.83	-		
N₂	7.70	71.55	88.1536		

Total air demand is calculated for 1 m³ mixed natural gas combustion. For $\lambda = 1$; 1 m³/h natural gas mixture needs 9.75 m³/h air theoretically.

Theoretical combustion equation and calculated wet and dry volumetric combustion products for $\lambda = 1.2$ are shown in **Table 3.11**.

Table 3.11: Theoretical combustion products calculations of mixed NG, $\lambda = 1.2$

Mixed Natural Gas Combustion Lambda=1.2							
						Composition	
1 CH ₄	+ 2.4 (1 O ₂ + 3.8 N ₂)	=	1 CO ₂	+ 2 H ₂ O	+ 9.024 N ₂	+ 0.4 O ₂	96.06
1 C ₂ H ₆	+ 4.2 (1 O ₂ + 3.8 N ₂)	=	2 CO ₂	+ 3 H ₂ O	+ 15.79 N ₂	+ 0.7 O ₂	2.133
1 C ₃ H ₈	+ 6 (1 O ₂ + 3.8 N ₂)	=	3 CO ₂	+ 4 H ₂ O	+ 22.56 N ₂	+ 1 O ₂	0.748
1 C ₄ H ₁₀	+ 7.8 (1 O ₂ + 3.8 N ₂)	=	4 CO ₂	+ 5 H ₂ O	+ 29.33 N ₂	+ 1.3 O ₂	0.233
Total Air Demand	11.70						m ³ /h
Combustion Products		Wet	Dry	Total Wet	12.714		m ³ /h
	m ³ /h	%	%	Total Dry	10.687		m ³ /h
CO ₂	1.04	8.14	9.68				
H ₂ O	2.03	15.94	-				
N ₂	9.24	72.70	86.4818				
O ₂	0.41	3.22	3.83341				

Total air demand is calculated for 1 m³ mixed natural gas combustion. For $\lambda = 1.2$; 1 m³/h natural gas mixture needs 11.7 m³/h air theoretically.

3.2.2 Geometry

Burner geometry has complicated parts due to the its design and operation principle. For CFD analysis burner geometry is simplified. Simplifications that are done in geometry is;

1. Ignition electrode and ionization electrode are not modelled,
2. Ignition electrode and ionization electrode mounting parts are not modelled,
3. Screws and connection holes are not modelled,
4. Burner body and other equipment are not used in modelled geometry,
5. Geometrical simplifications are done in diffuser wings,
6. Fixing plate of the flame tube extension is not modelled.

Burner and boiler geometries are modelled by using Solidworks software. Burner geometry consists of flame tube, flame tube extension, gas pipe, combustion head-gas nozzles, inner and outer diffuser which are shown in **Figure 3.14**.

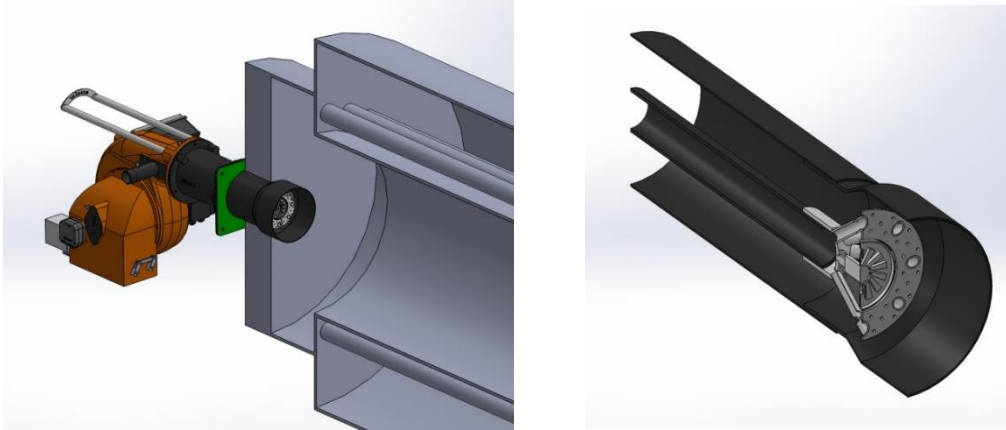


Figure 3.14: Burner geometry and CFD burner geometry

Burner and first combustion chamber geometry; geometry-1 is shown in **Figure 3.15**.

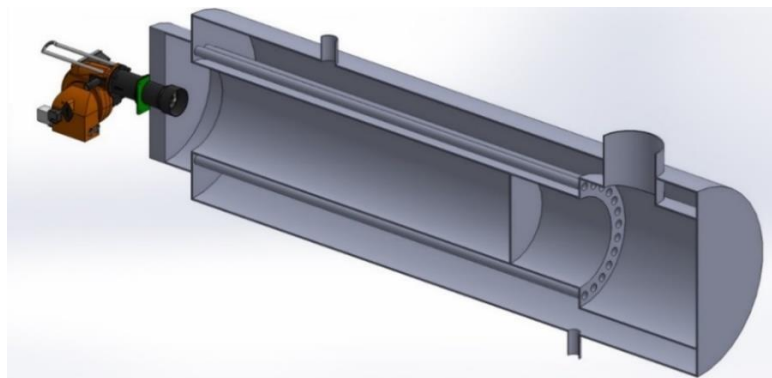


Figure 3.15: Geometry-1

Burner and second combustion chamber geometry; geometry-2 is shown in **Figure 3.16**.

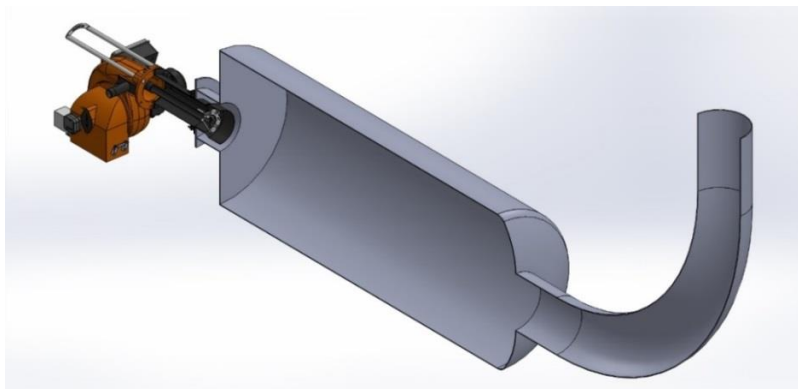


Figure 3.16: Geometry-2

Simplified burner and boiler geometries are imported to Ansys Design Modeler so that fluid volume for CFD solutions is generated. Imported first geometry is shown in **Figure 3.17**.

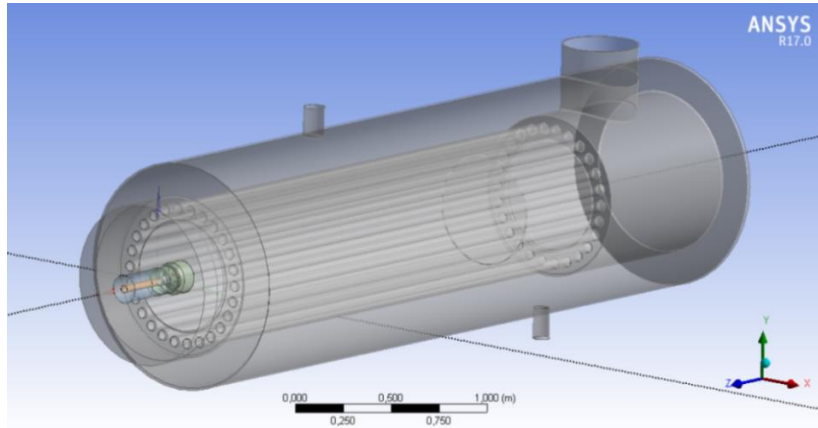


Figure 3.17: Imported first burner and boiler geometry

Fluid volume is created in ANSYS Design Modeler and arranged before meshing to increase mesh quality and decrease element number. Fluid volumes of the first geometry-numerical studies are shown in **Figure 3.18** and **Figure 3.19**.

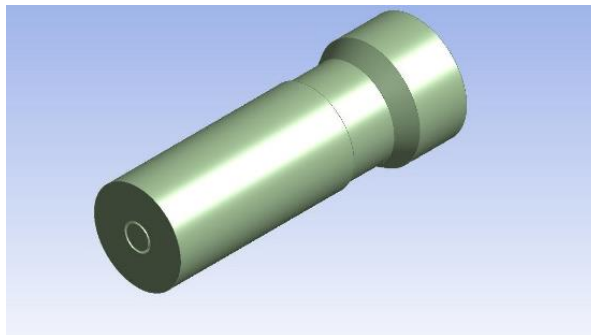


Figure 3.18: Fluid volume of numerical studies of the burner geometry

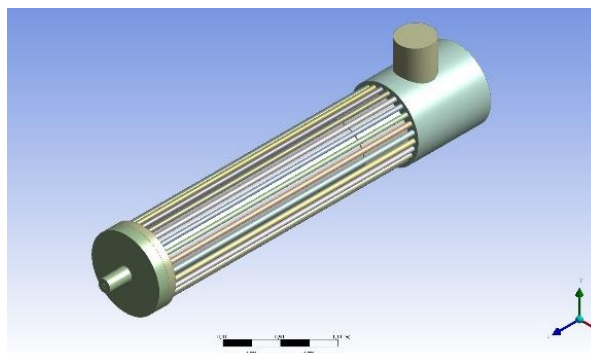


Figure 3.19: Fluid volume of numerical studies of the first geometry

Imported second geometry of numerical studies is shown in **Figure 3.20**.

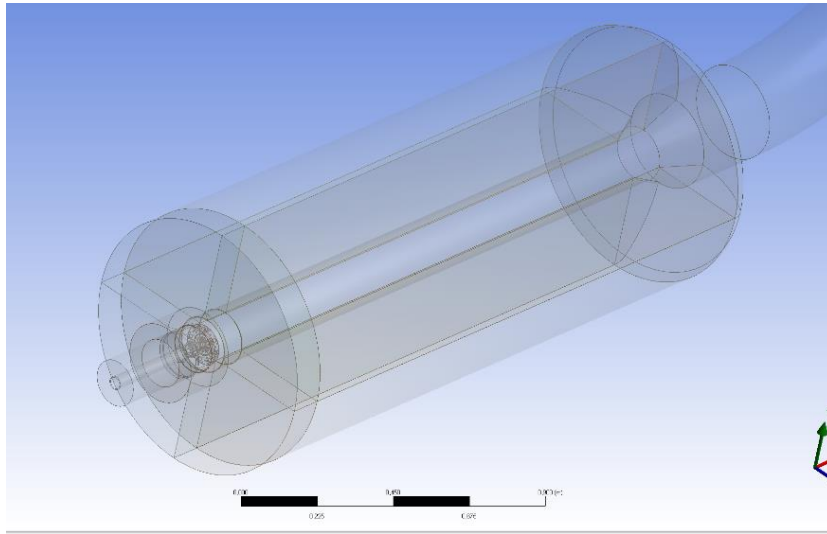


Figure 3.20: Imported second burner and boiler geometry

Fluid volume of the second geometry-numerical studies are shown in **Figure 3.21**.

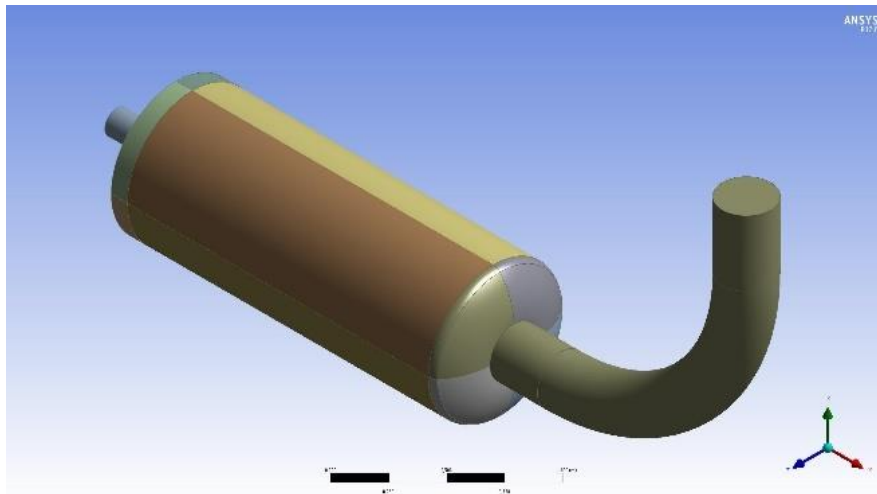


Figure 3.21: Fluid volume of numerical studies of the second geometry

3.2.3 Mesh Independency and Cold Flow Studies

Mesh independency studies are done with four different meshed geometries that are prepared to find the suitable quality and mesh element number. Details of the burner combustion head are directly affected the mesh quality and mesh number. During the mesh independency studies, element sizes in burner head and related combustion chamber parts where the combustion occurs, are changed to improve mesh quality.

In **Table 3.12** mesh details of first geometry that is used in mesh independency studies are shown.

Table 3.12: Mesh element number and mesh quality of the first geometry

Mesh Name	Element Number	Skewness (Maksimum)	Orthogonal Quality (Minimum)
Mesh-1	5961246	0.84834	0.22609
Mesh-2	5522284	0.87171	0.21169
Mesh-3	4789363	0.89912	0.18363
Mesh-4	4399183	0.93495	0.08915

For the first geometry, cold flow analysis done for the four-different mesh option with following conditions listed in **Table 3.13**.

Table 3.13: Cold flow analysis studies solution conditions

Fuel	Mix natural gas
Gas Consumption [Nm ³ /h]	125.1
Excess Air (λ)	1.2

Cold flow analysis comparison graph for the first geometry is shown in **Figure 3.22**. Velocities in axial direction of the combustion chamber are compared for four-different meshed geometries.

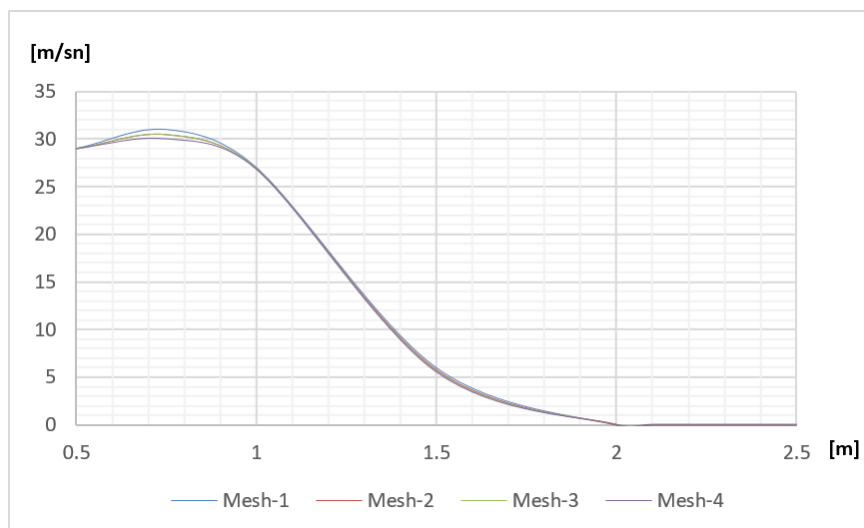


Figure 3.22: Axial Velocity [m/s] versus position [m]

Mesh-3 is found accurate enough for further studies. Mesh-3 is used for the numerical studies. Details of Mesh-3 are shown in **Figure 3.23** and **Figure 3.24**.

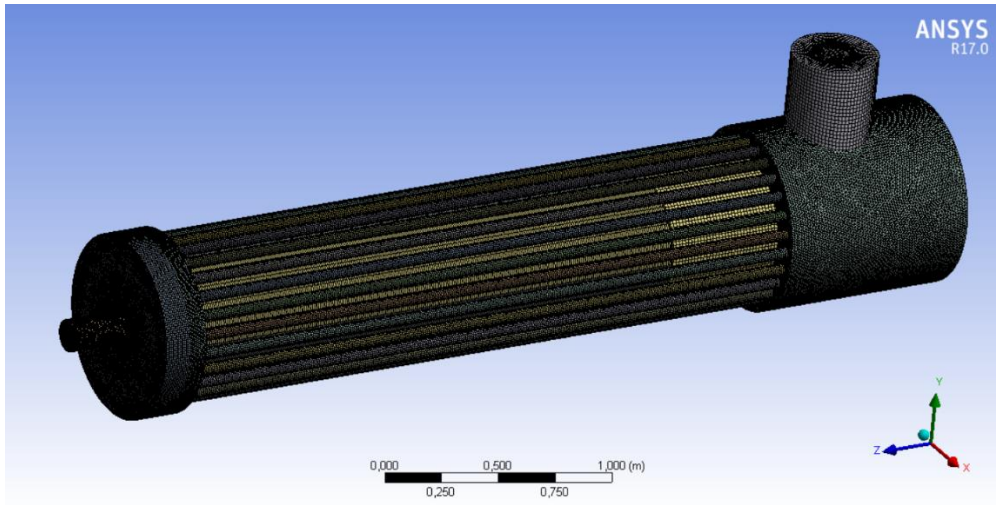


Figure 3.23: Details of Mesh-3 for the first geometry

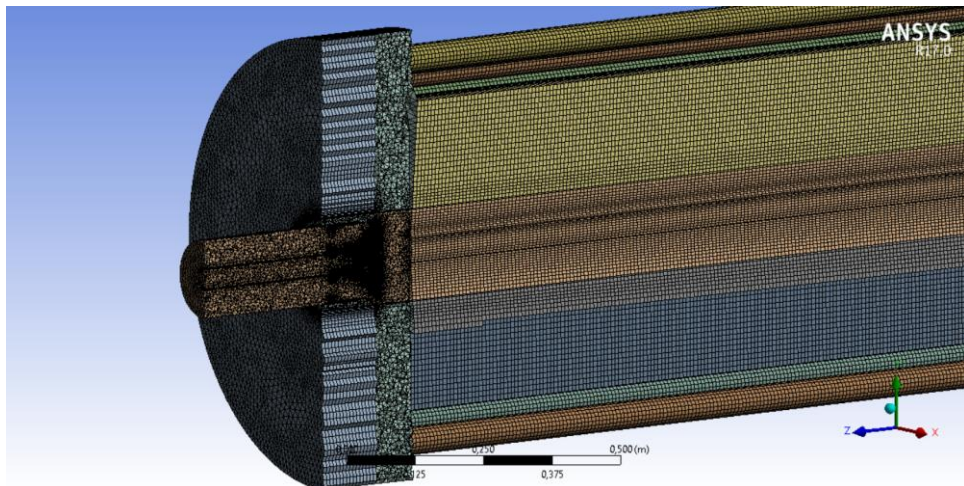


Figure 3.24: Details of Mesh-3 for the first geometry

Similar mesh method is used for the second geometry and selected mesh details of the second geometry are shown in **Table 3.14**, **Figure 3.25**.

Table 3.14: Mesh element number and mesh quality of the second geometry

Mesh Name	Element Number	Skewness (Maksimum)	Orthogonal Quality (Minimum)
Mesh	1765171	0,87745	0,15717

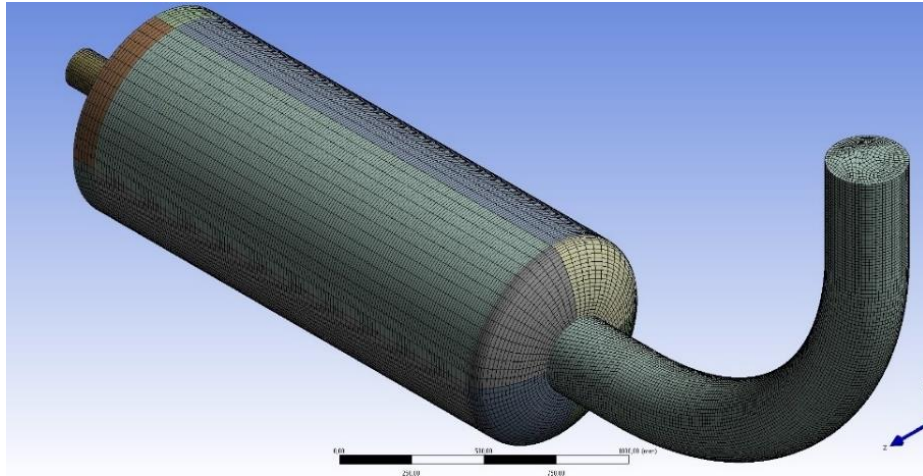


Figure 3.25: Mesh details of the second geometry

3.2.4 Boundary Conditions

Mass flow inlet boundary condition is used for both fuel inlet and air inlet during the numerical studies. Pressure outlet boundary condition is defined for the outlet. Boundary conditions of the first geometry are shown in **Figure 3.26**.

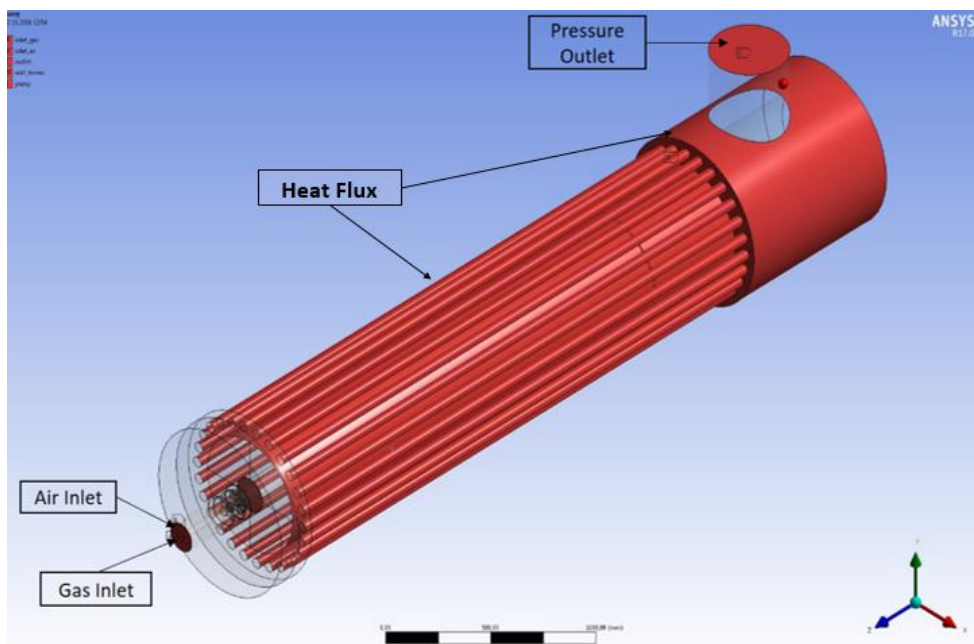


Figure 3.26: Named selection of boundary conditions for the first geometry

Mass flow inlet boundary condition is used for both fuel inlet and air inlet during the numerical studies. Wall temperature and pressure outlet boundary condition is defined for the outlet. Boundary conditions of the second geometry are shown in **Figure 3.27**.

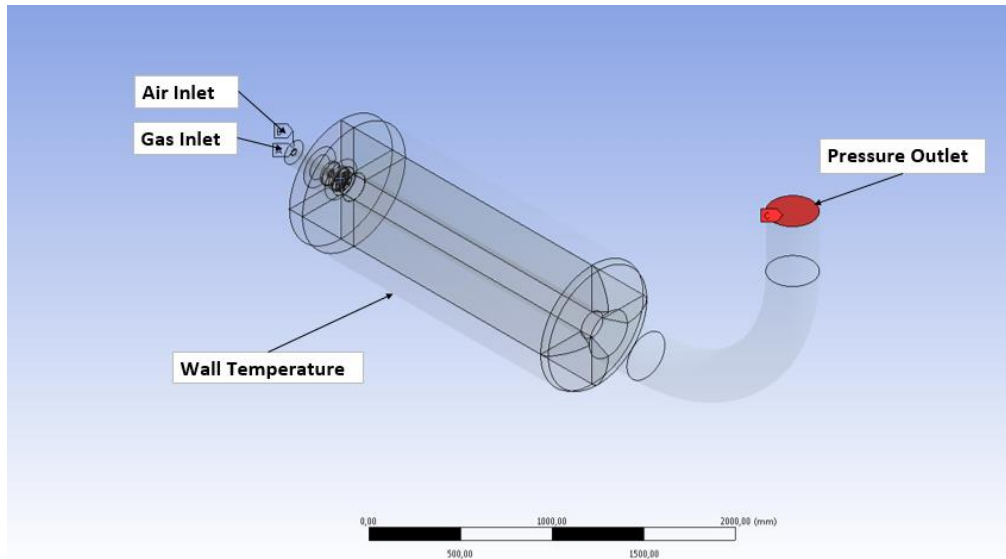


Figure 3.27: Named selection of boundary conditions for the second geometry

In numerical studies **100% methane** and **mix natural gas** are used. Mix natural gas composition and LHV-HHV calculations of mix natural gas are shown in **Table 3.15.** [24-26]

Table 3.15: LHV and HHV calculations of mix natural gas

	Composition Percentage	LHV	HHV
	%	kJ/m³	kJ/m³
Methane	96.064	33948	37706
Ethane	2.133	60430	66070
Propane	0.748	86420	93940
İ-Bütane	0.115	112400	121790
N-Bütane	0.118	112010	121400
Nitrogen	0.659	-	-
Carbon dioxide	0.163	-	-
Heating Value		8313.90	9223.55
Compression Factor		0.9981	0.9981
Heating Value	kcal/m ³	8329.73	9241.11

Boundary condition calculations for the fuel and air mass flow inlet are done and calculated values are shown in **Table 3.16.**

Table 3.16: Mass flow inlet of the fuel and air boundary condition calculations for %100 CH4 and mix natural gas combustion.

%100 CH4 $\lambda=1$		
Gas Consumption	125.1	Nm ³ /h
Gas Density	0.68	kg/Nm ³
Gas Consumption	85.068	kg/h
	0.02363	kg/sn
Air Consumption	1190.952	m ³ /h
Air Density	1.225	kg/m ³
Air Consumption	1458.916	kg/h
	0.405255	kg/sn

%100 CH4 $\lambda=1.2$		
Gas Consumption	125.1	Nm ³ /h
Gas Density	0.68	kg/Nm ³
Gas Consumption	85.068	kg/h
	0.02363	kg/sn
Air Consumption	1429.142	m ³ /h
Air Density	1.225	kg/m ³
Air Consumption	1750.699	kg/h
	0.486305	kg/sn

Mix Natural Gas $\lambda=1$		
Gas Consumption	125.1	Nm ³ /h
Gas Density	0.711	kg/Nm ³
Gas Consumption	88.9461	kg/h
	0.024707	kg/sn
Air Consumption	1219.821	m ³ /h
Air Density	1.225	kg/m ³
Air Consumption	1494.28	kg/h
	0.415078	kg/sn

Mix Natural Gas $\lambda=1.2$		
Gas Consumption	125.1	Nm ³ /h
Gas Density	0.711	kg/Nm ³
Gas Consumption	88.9461	kg/h
	0.024707	kg/sn
Air Consumption	1463.785	m ³ /h
Air Density	1.225	kg/m ³
Air Consumption	1793.136	kg/h
	0.498093	kg/sn

Hydraulic diameter is a commonly used characteristic length to deal in non-circular tube and channel flows. Hydraulic diameter can be calculated with following equations;

$$d_h = 4 * \frac{A}{P} \text{ (eq number)} \quad (3.1)$$

d_h : Hydraulic diameter A: Area of the section P: Wetted perimeter

Table 3.17: Calculated hydraulic diameter for the fuel and air mass flow inlet boundary conditions

Flame Tube Inner Diameter	0.144	m
Gas Tube Outer Diameter	0.0424	m
Gas Tube Inner Diameter	0.0359	m
Hydraulic Diameter for Fuel	0.0359	m
Hydraulic Diameter for Air	0.1016	m

3.2.5 Reactive Analysis

Reactive analyses are performed for two different combustion chamber geometries with the same burner geometry. Firstly, the combustion chamber geometry is water-cooled so that experiments at different loads are able to be done. Secondly, the combustion chamber geometry is uncooled, due to the thermal loads and temperature limitations, experiments are conducted for only low-load conditions.

Turbulent flow was modelled by using **k-ε turbulent model**. **PDF-Flamelet** combustion model and **DO** radiation model were used during the numerical studies. **Mass flow inlet** was used for the both fuel and air inlet conditions. Constant **wall temperature** was defined for the outer shells of the test combustion chamber (SCC) and the calculated **heat flux** is defined for the hot-water boiler (FCC) due to unknown wall temperature. **Pressure outlet** boundary condition was defined as outlet boundary condition.

First reactive analysis case studies were done in different excess air values for high load. For the mixed natural gas and %100 methane; 125.1 Nm³/h gas consumption case study results are shown in **Table 3.18**.

Table 3.18: Reactive analysis results for the mixed natural gas and %100 methane for 125.1 Nm³/h gas consumption in different excess air values for the first geometry.

Case	Fuel Type	λ	O ₂	CO ₂	NO _x
		-	%	%	ppm
Case-1	Mix Natural Gas	1.1	1.61	10.7	61.2
Case-2	Mix Natural Gas	1.2	3.3	9.6	61.6
Case-3	Mix Natural Gas	1.3	4.26	9.03	53.32
Case-4	Mix Natural Gas	1.4	5.61	8.11	55.53
Case-5	%100 Methane	1.2	3.25	9.56	55.52

Reactive analysis contours such as mole fraction of CO₂, mole fraction of O₂, static temperature and nitrogen oxide for the mix natural gas and 100% in 125.1 Nm³/h gas consumption with $\lambda=1.2$ that is commonly used excess air value for the natural gas combustion in industrial applications for the first geometry are shown between **Figure 3.28 and Figure 3.31**.

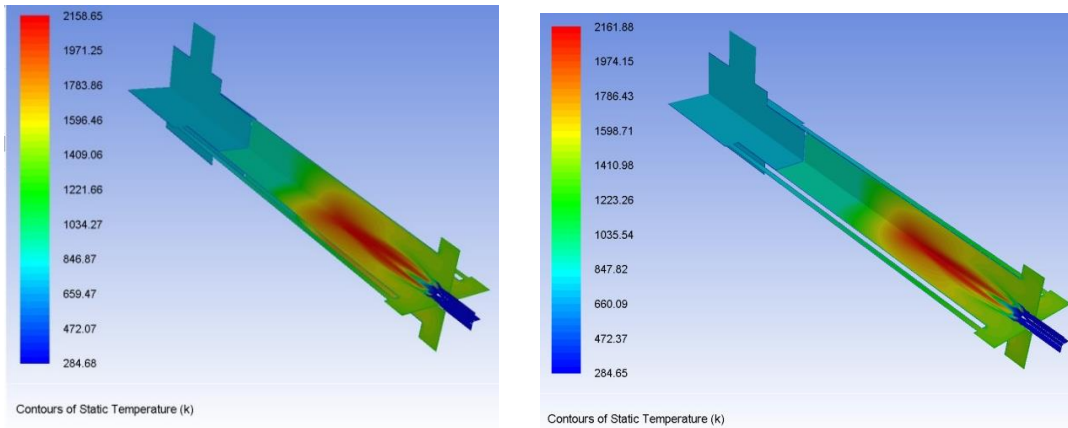


Figure 3.28: Temperature [K] contour plots of the first geometry for NG and Methane

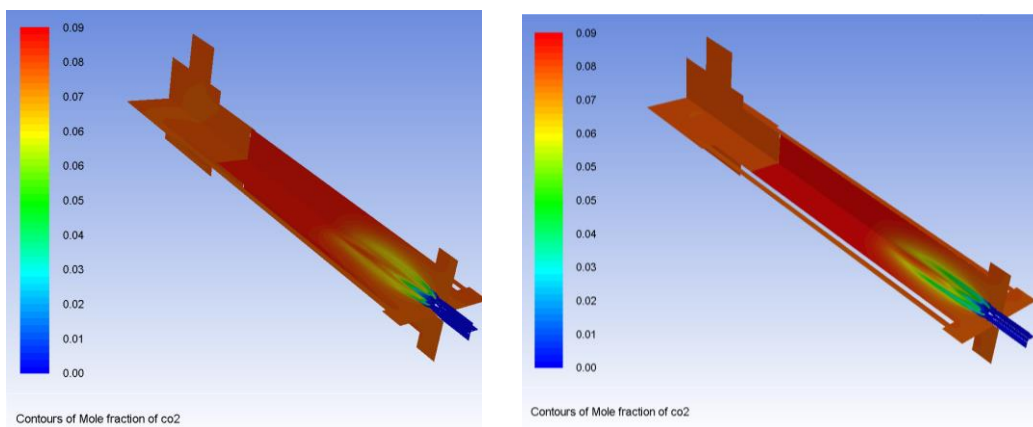


Figure 3.29: CO₂ [%] contour plots of the first geometry for NG and Methane

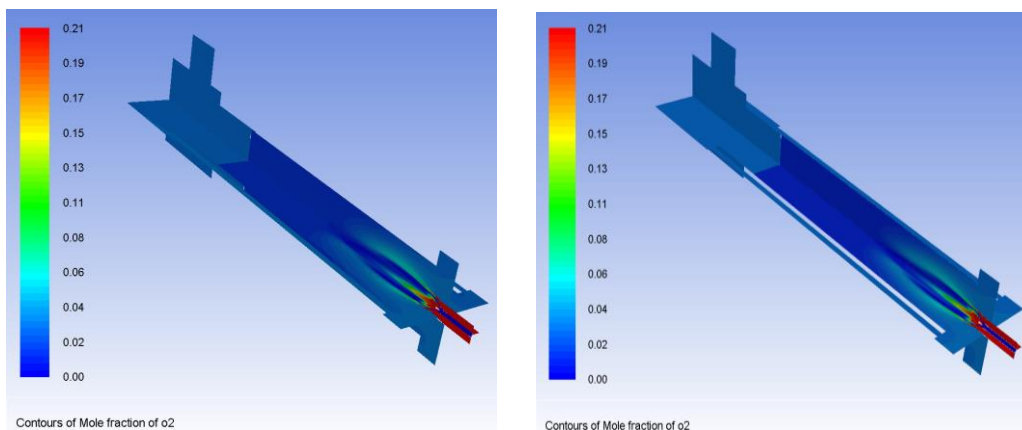


Figure 3.30: O₂ [%] contour plots of the first geometry for NG and Methane

Numerically it is observed that temperature distribution and CO₂, O₂ values are similar when %100 methane and mix natural gas are compared. However calculated NO_x value is shown ~6 ppm difference for the mix natural and 100% methane.

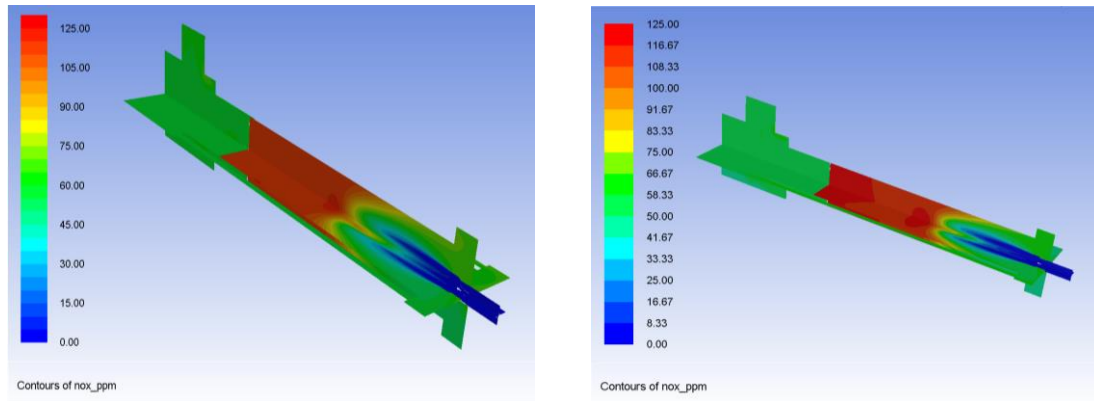


Figure 3.31: NO_x [ppm] contour plot of the first geometry for NG and Methane Reactive analysis contours such as mole fraction of CO_2 , mole fraction of O_2 , static temperature, velocity magnitude and nitrogen oxide for the mix natural gas in $125.1 \text{ Nm}^3/\text{h}$ gas consumption for different excess air values are shown in **Figure 3.32**.

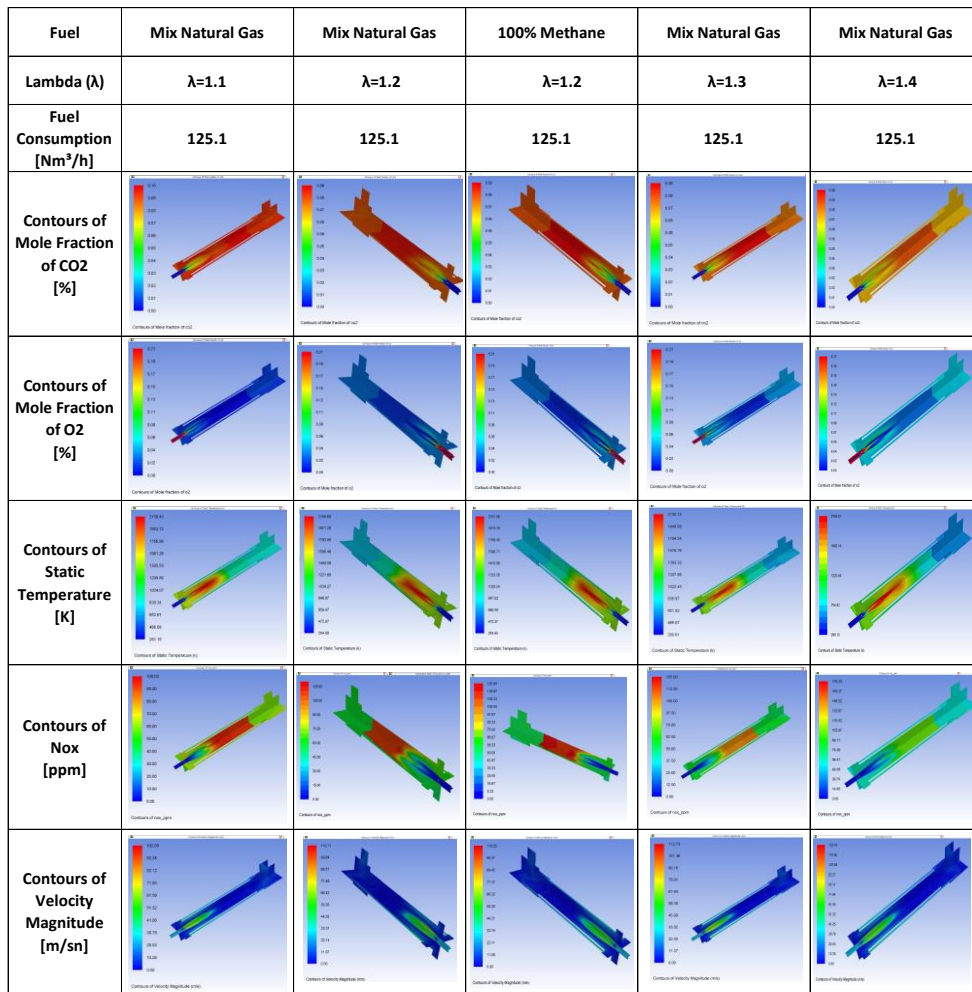


Figure 3.32: Contour plots of the numerical study results for the first geometry

Second reactive analysis case studies were done in the same excess air value; $\lambda=1.2$, for different burner loads. Reactive analysis contours such as mole fraction of CO_2 , mole fraction of O_2 , static temperature, velocity magnitude and nitrogen oxide for the mixed natural gas are shown in **Figure 3.33**.

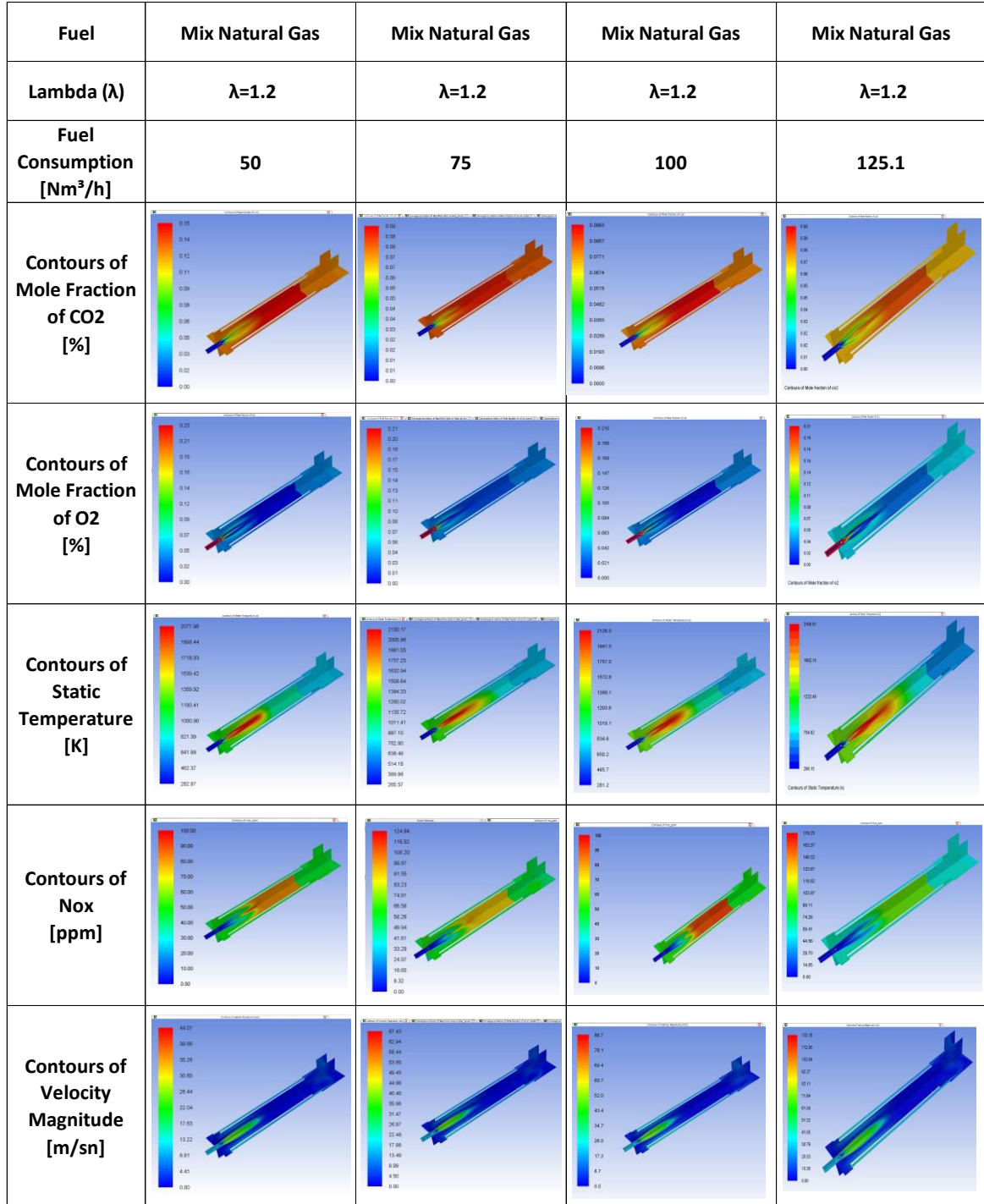


Figure 3.33: Contour plots of the numerical study results for the first geometry

Second reactive analysis case study results for the first geometry are shown in **Table 3.19**.

Table 3.19: Reactive analysis results for the mix natural gas for $\lambda=1.2$ for the first geometry.

Case	Fuel Type	Gas Consumption	λ	O_2	CO_2	NO_x
		Nm ³ /h	-	%	%	ppm
Case-6	Mix Natural Gas	50	1.2	3.5	9.48	46.54
Case-7	Mix Natural Gas	75	1.2	3.5	9.83	56.86
Case-8	Mix Natural Gas	100	1.2	3.5	9.50	49.7
Case-2	Mix Natural Gas	125	1.2	3.3	9.60	61.6

The results of the Case-2, Case-6, Case-7 and Case-8; CO_2 emission values are compared in Table 3.19. It is observed that results are nearly same with the difference of $\Delta[\%] = 2.5$; NO_x values are found more about $\sim\Delta[\text{ppm}] = 14$ ppm.

Third reactive analysis case study was done for the mixed natural gas in 35 Nm³/h gas consumption for the second geometry for $\lambda=1.3$. Reactive analysis results are shown in **Table 3.20**.

Table 3.20: Reactive analysis results for the mix natural gas in 35 Nm³/h gas consumption for the second geometry in $\lambda=1.3$.

	λ	O_2	CO_2	NO_x
		%	%	ppm
Case-9	1.3	4.9	8.84	56

Reactive analysis contours such as mole fraction of CO_2 , mole fraction of O_2 , static temperature and nitrogen oxide for the mix natural gas in 35 Nm³/h gas consumption, $\lambda=1.3$ are shown between **Figure 3.34 and Figure 3.37**. Due to the non-cooling walls of the combustion chamber geometry, there is not such a big temperature difference inside the combustion chamber and flue part.

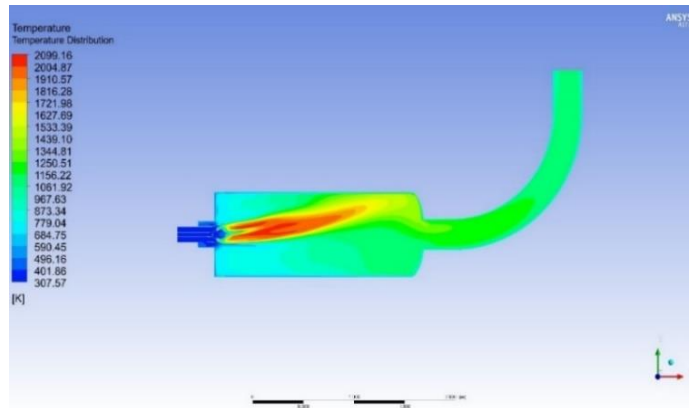


Figure 3.34: Temperature [K] contour plot of the second geometry

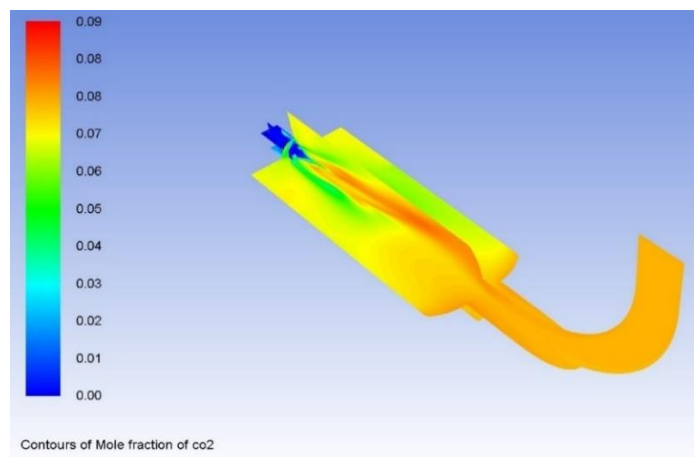


Figure 3.35: CO₂ [%] contour plot of the second geometry

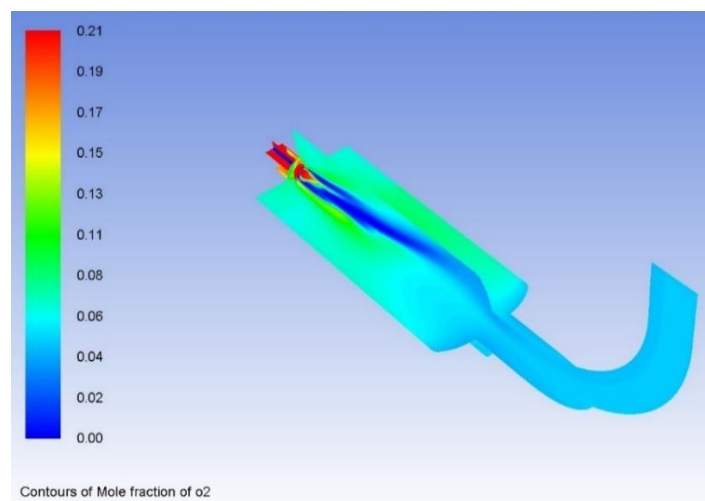


Figure 3.36: O₂ [%] contour plot of the second geometry

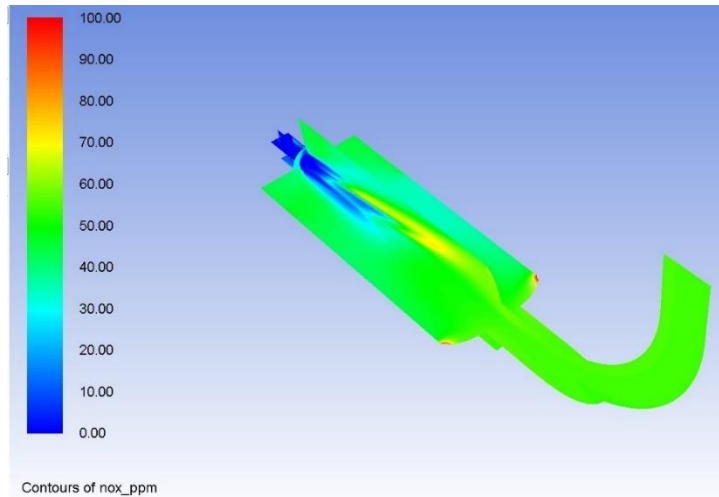


Figure 3.37: NO_x [ppm] contour plot of the second geometry

3.2.6 Comparison of Numerical and Experimental Studies

The comparison of numerical and experimental studies for the **first reactive analysis case studies** for natural gas are shown in **Table 3.21** and **Figure 3.38 - Figure 3.40**. Differences in experiments and numerical studies are found to be $\Delta O_2 \sim 7\%$, $\Delta CO_2 \sim 2\%$, $\Delta NO_x \sim 12\%$. Mix natural gas numerical study results are closer when compared with the methane case study to the experimental results.

Table 3.21: Numerical studies and experimental studies comparison of the **first reactive analysis case studies and experiments**

Case Experiment	Fuel Type	Gas Consumption	λ	O ₂	CO ₂	NO _x
		Nm ³ /h	-	%	%	ppm
Case-1	Mix Natural Gas	125.1	1.1	1.61	10.7	61.2
Experiment-1	Mix Natural Gas	125.1	1.1	2	10.41	66
Case-2	Mix Natural Gas	125.1	1.2	3.3	9.6	61.6
Experiment-2	Mix Natural Gas	125.1	1.2	3.5	9.76	63
Case-3	Mix Natural Gas	125.1	1.3	4.26	9.03	53.32
Experiment-3	Mix Natural Gas	125.1	1.3	4.9	8.77	57
Case-4	Mix Natural Gas	125.1	1.4	5.61	8.11	55.53
Experiment-4	Mix Natural Gas	125.1	1.4	6	8.18	51

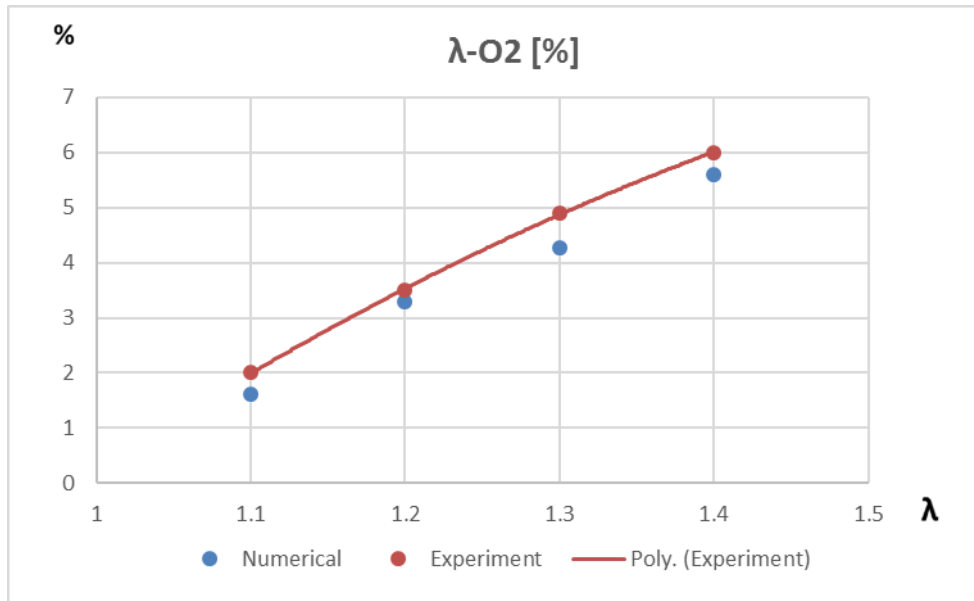


Figure 3.38: Lambda versus oxygen [%]

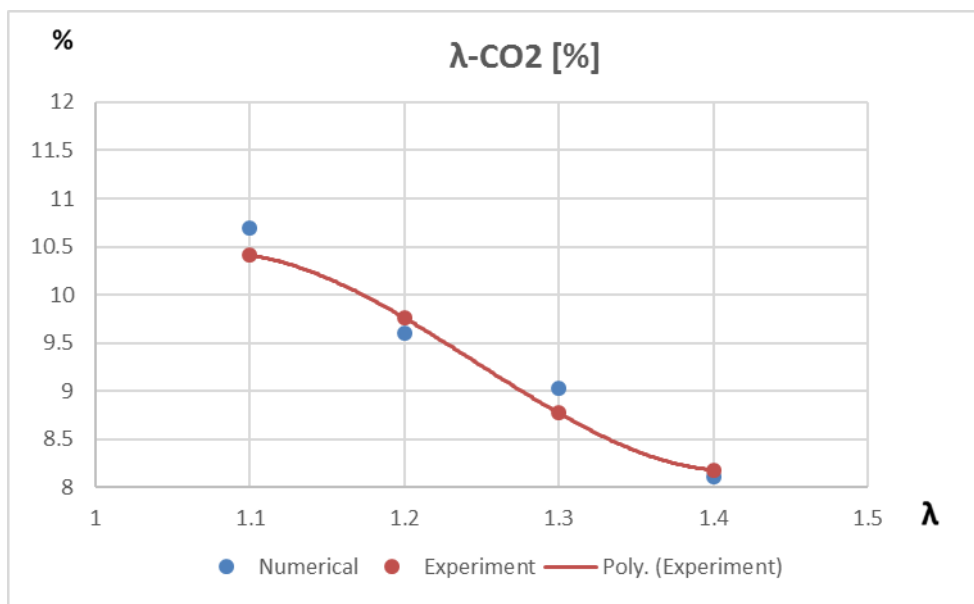


Figure 3.39: Lambda versus carbon dioxide [%]

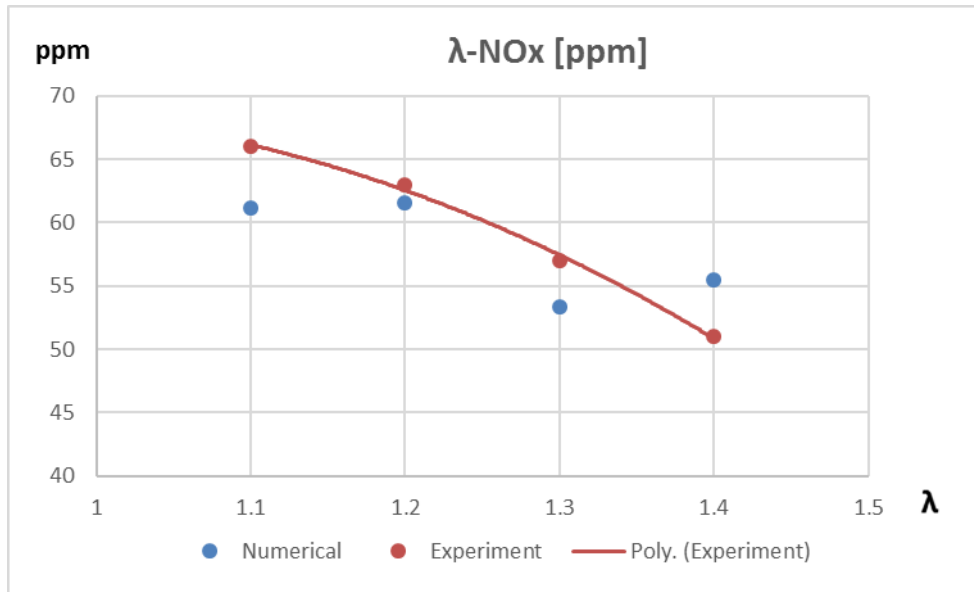


Figure 3.40: Lambda versus nitrogen oxide [ppm]

Numerical studies and experimental studies are compared for the **second reactive analysis case studies** for natural gas. Results are shown in **Table 3.22** and **Figure 3.41 - Figure 3.43**. Differences in experiments and numerical studies are found to be $\Delta O_2 \sim 5\%$, $\Delta CO_2 \sim 2\%$, $\Delta NO_x \sim 18\%$.

Table 3.22: Numerical studies and experimental studies comparison of the **second reactive analysis case studies and experiments**

Case Experiment	Fuel Type	Gas Consumption	λ	O2	CO2	NOx
		Nm ³ /h	-	%	%	ppm
Case-6	Mix Natural Gas	50	1.2	3.5	9.48	46.54
Experiment-6	Mix Natural Gas	50	1.2	3.5	9.44	57
Case-7	Mix Natural Gas	75	1.2	3.5	9.83	56.86
Experiment-7	Mix Natural Gas	75	1.2	3.4	9.72	65
Case-8	Mix Natural Gas	100	1.2	3.5	9.50	49.7
Experiment-8	Mix Natural Gas	100	1.2	3.5	9.55	61
Case-2	Mix Natural Gas	125.1	1.2	3.3	9.6	61.6
Experiment-2	Mix Natural Gas	125.1	1.2	3.5	9.76	63

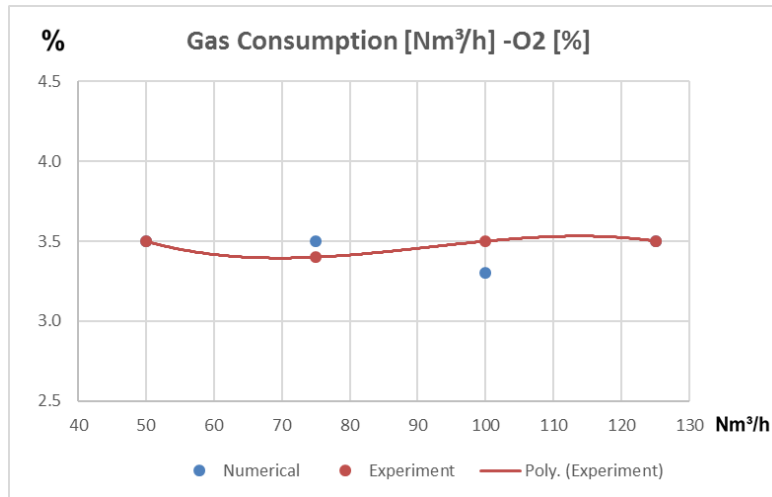


Figure 3.41: Gas consumption [Nm³] versus oxygen [%]

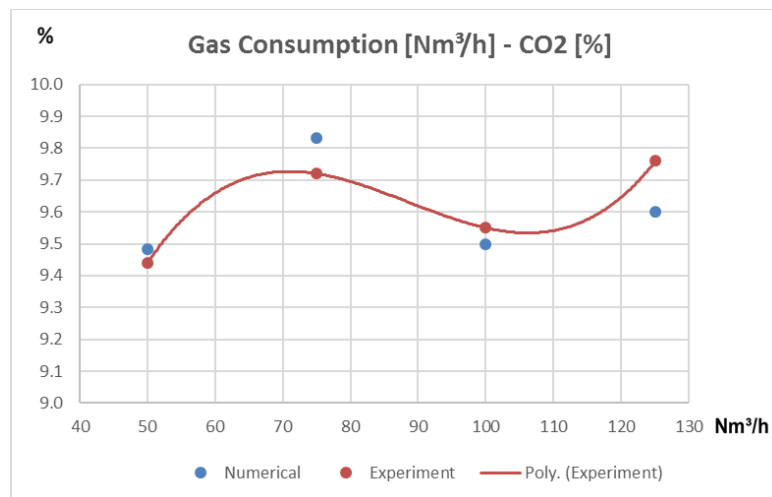


Figure 3.42: Gas consumption [Nm³] versus carbon dioxide [%]

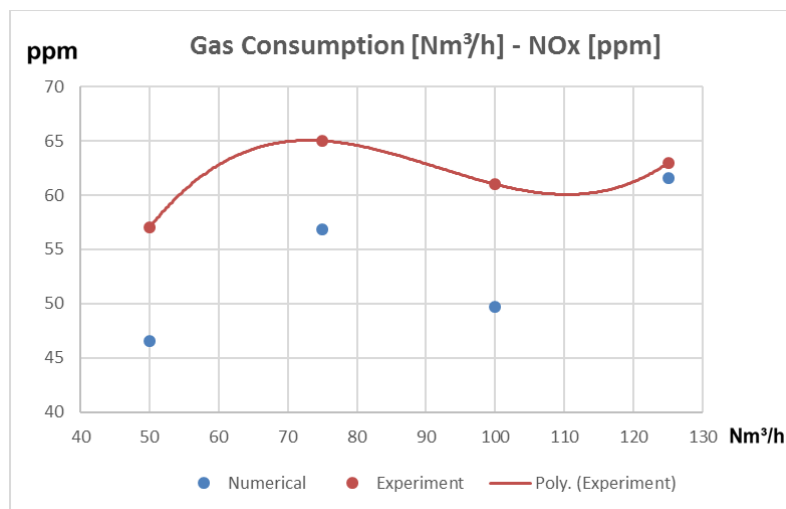


Figure 3.43: Gas consumption [Nm³] versus nitrogen oxide [ppm]

Numerical studies and experimental studies comparison for the **third reactive analysis case study** for natural gas are shown in **Table 3.23**. Differences in experiments and numerical studies are found to be $\Delta O_2 \sim 0.62\%$, $\Delta CO_2 \sim 2\%$, $\Delta NO_x \sim 2.5\%$. Experiment and numerical study comparisons show that when the measured wall temperature was defined as a wall temperature boundary condition, especially numerical NO_x values are closer to experimental measured values.

Table 3.23: Numerical studies and experimental studies comparison for the second geometry

Case Experiment	Fuel	Fuel Flow Rate	O ₂	CO ₂	NO _x
	-	Nm ³ /h	%	%	ppm
Case-9	Mix Natural Gas	35	4.9	8.84	56
Experiment-9	Mix Natural Gas	35	4.87	8.65	54.76
Difference [$\Delta\%$]	-	-	0.62	2.20	2.26

3.2.7 Geometry Modifications to Achieve Low NO_x Emission

Two new geometry was modelled and numerically simulated with aim of decreasing NO_x emission.

New Geometry-1 (NG-1) was modelled to see how flame tube extension affect the flame shape and modifications were done for gas nozzles, nozzle shape modified with radius form to decrease pressure lost. Modelled geometry, NG-1 is shown in **Figure 3.44**.

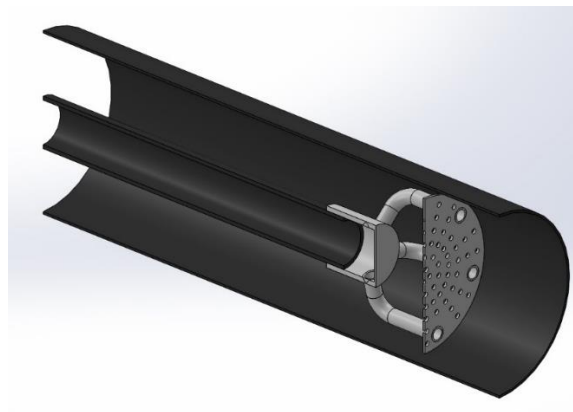


Figure 3.44: New Geometry-1

With modified gas nozzles pressure lost inside the combustion head was improved but without flame tube extension flame shape was unacceptable and need modifications to make flame rounded and longer. Temperature contour of NG-1 is shown in **Figure 3.45**.

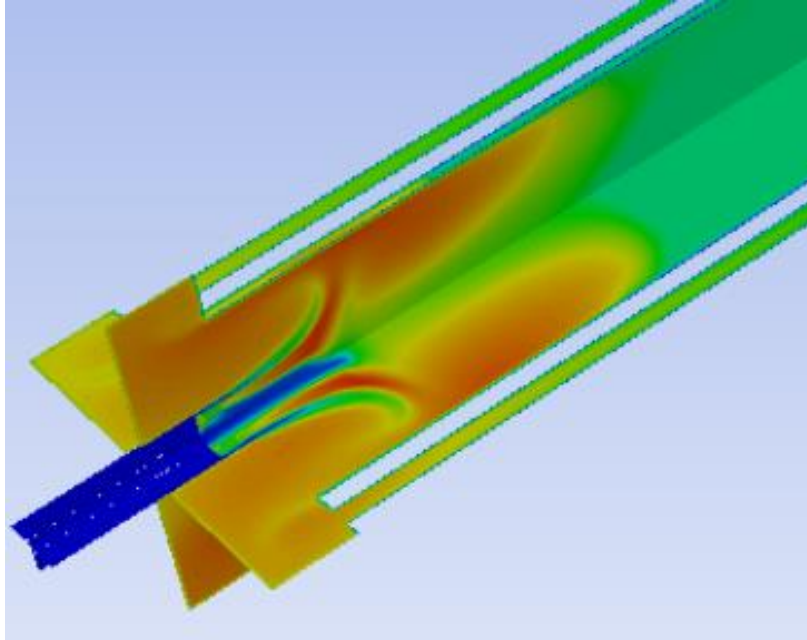


Figure 3.45: Temperature contour of New Geometry-1

NG-1 was modified and New Geometry-2 (NG-2) was modelled. Modified gas nozzle shape was used and gas outlets were added in the center of the combustion head (1). Conical part (2) was added to flame tube to improve flame shape. NG-2 is shown in **Figure 3.46**.

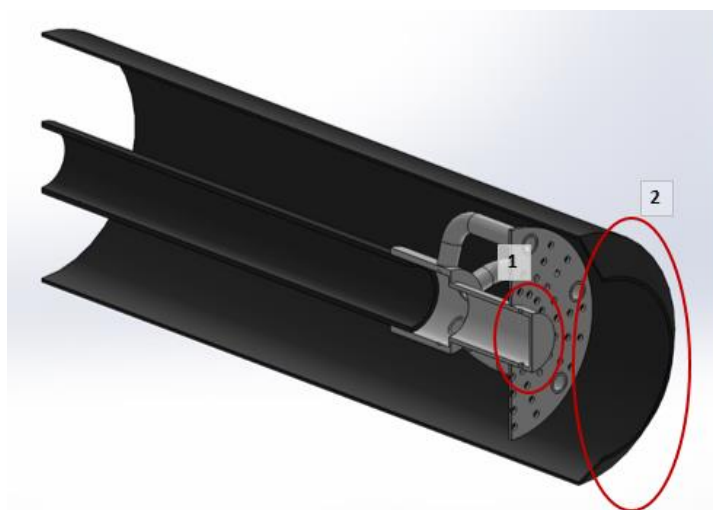


Figure 3.46: New Geometry-2

Mesh details of NG-2 is shown in **Figure 3.47** and **Figure 3.48**. Geometry has 2070285 element number and 0.87 maximum skewness value.

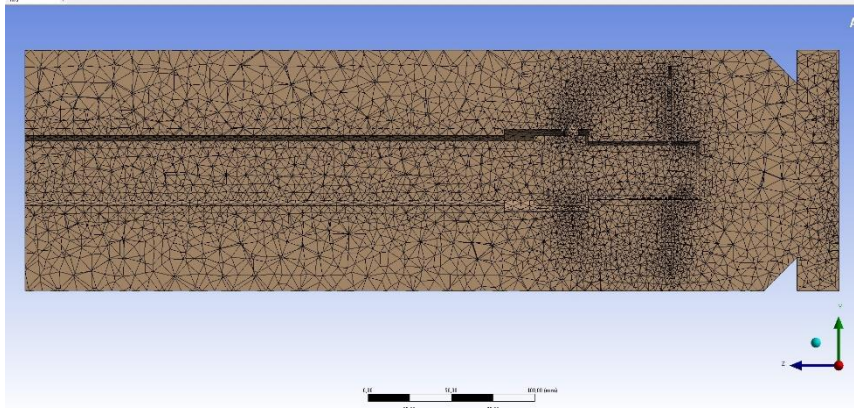


Figure 3.47: Mesh details of the NG-2 burner part

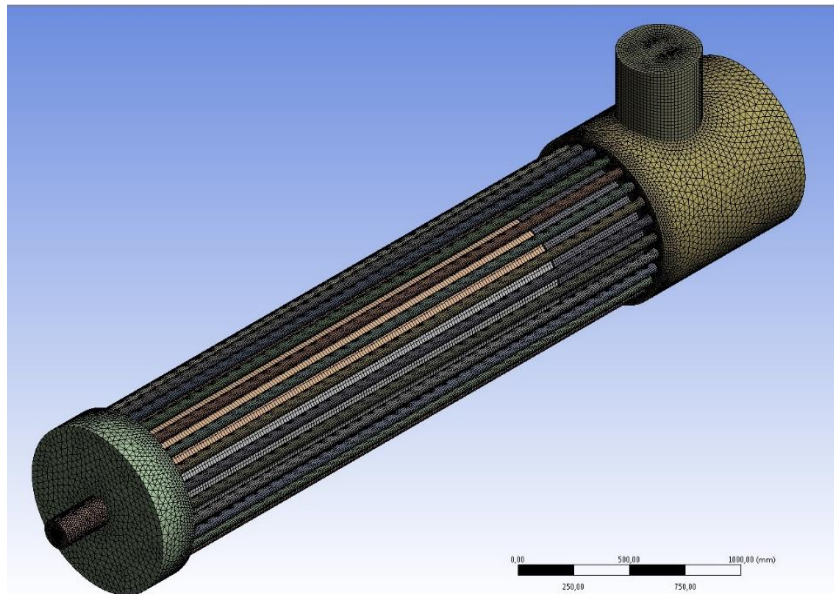


Figure 3.48: Mesh details of the NG-2

Reactive analysis case study was done for the mixed natural gas in 125.1 Nm³/h gas consumption for the NG-2 for $\lambda=1.2$. Reactive analysis result is shown in **Table 3.24**.

Table 3.24: Reactive analysis results for the mix natural gas in 125.1 Nm³/h gas consumption for the NG-2 in $\lambda=1.2$.

	λ	O ₂	CO ₂	NO _x
		%	%	ppm
Case-11	1.2	3.58	9.45	34.93

Reactive analysis contours such as mole fraction of CO₂, mole fraction of O₂, static temperature and nitrogen oxide for the mix natural gas in 125.1 Nm³/h gas consumption, $\lambda=1.2$ are shown between **Figure 3.49** and **Figure 3.52**.

Compared to New Geometry-1, flame is longer similar to original geometry length. Center of the flame is hotter compare the outer surface of the flame.

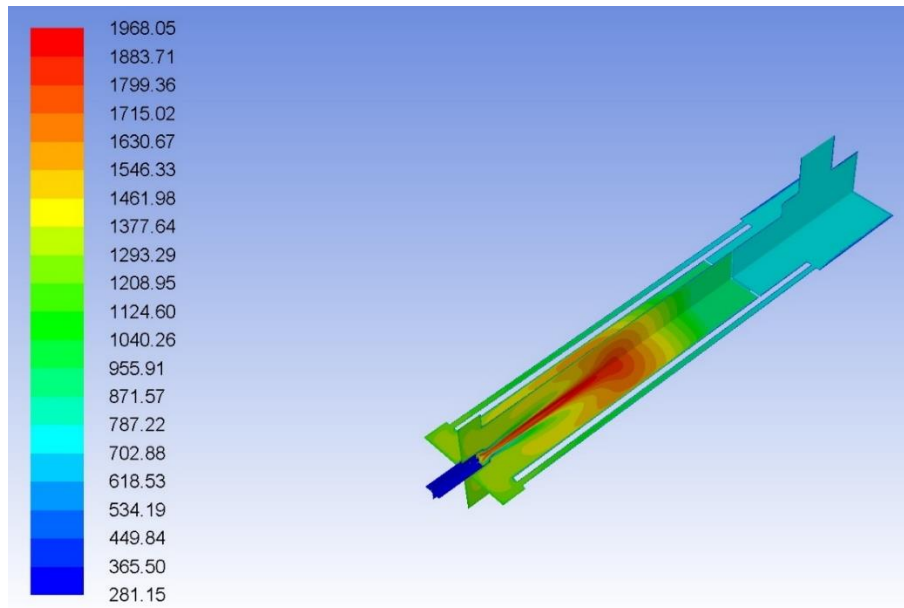


Figure 3.49: Temperature [K] contour plot of the NG-2

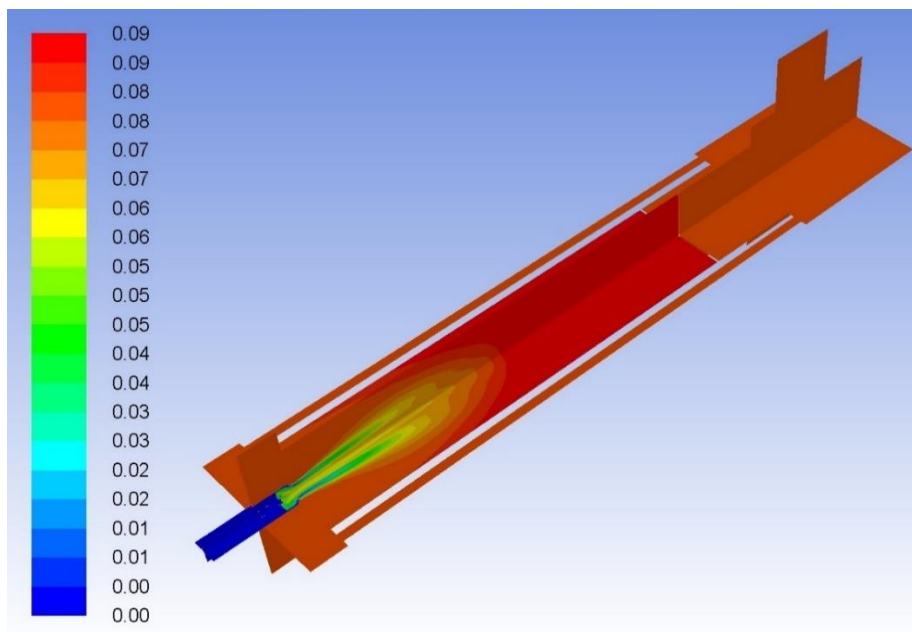


Figure 3.50: CO₂ [%] contour plot of the NG-2

Due to the added conical part and modified combustion head geometry combustion air is divided to two streams. Most of the combustion air is gone to center of the diffuser and some amount of combustion air is gone to outer surface of the flame. Flame is cooled with that way.

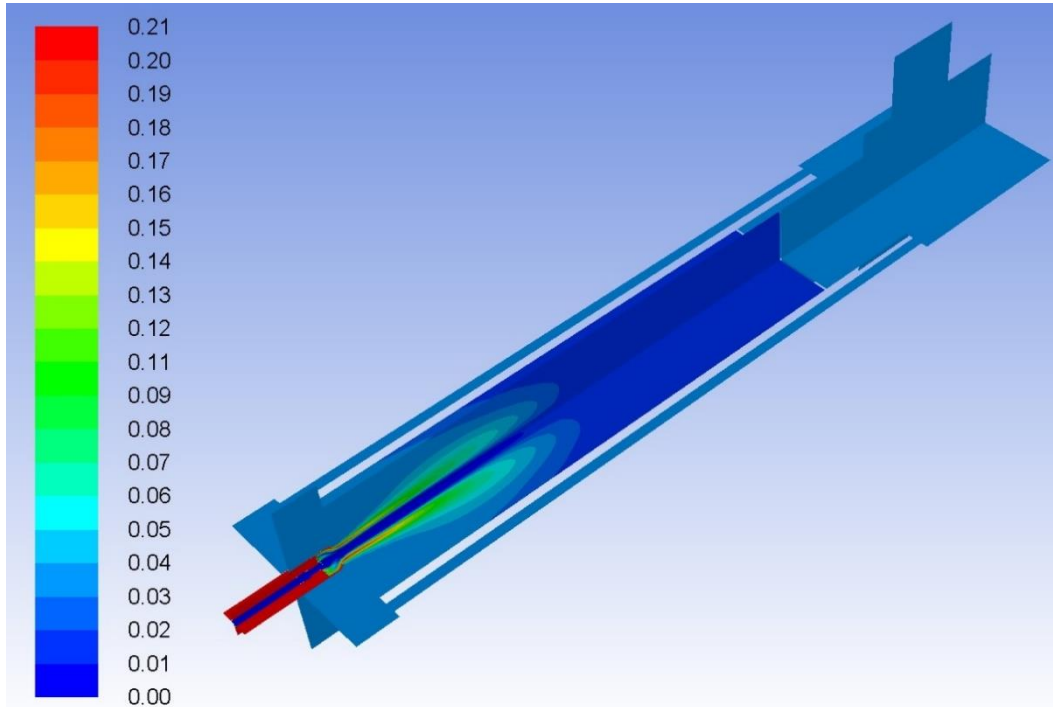


Figure 3.51: O₂ [%] contour plot of the NG-2

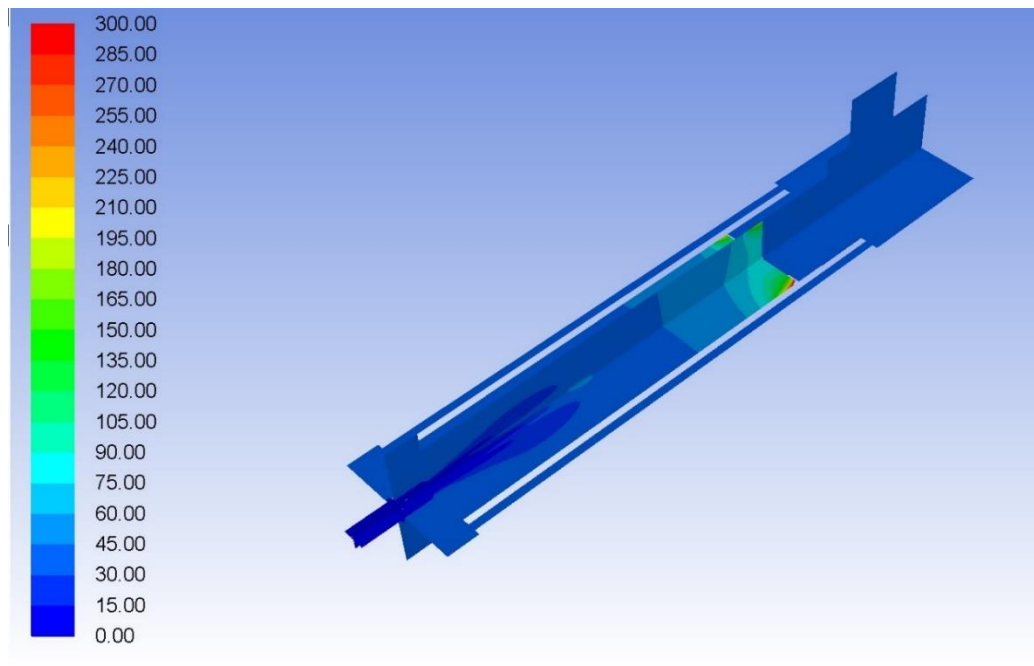


Figure 3.52: NO_x [ppm] contour plot of the second geometry

4. CONCLUSIONS

The numerical studies of a burner and modified burner geometries have been performed in this study. The numerical studies have been performed initially for the mesh independency. The accurate enough mesh number and size have been determined by comparing four mesh cases. Then reactive case studies have been performed with this mesh.

In reactive case studies, two different boiler geometries and three different burner geometry have been tried in 11 case studies. The results of reactive studies are examined in terms of contour plots including mole fractions of the emissions, NO_x , CO_2 , O_2 and static temperatures. Several equivalence ratios and loads were studied.

In the first reactive analyses and experiments which were done with mix natural gas and 100% methane. Numerically it is observed that temperature distribution and CO_2 , O_2 values are similar when %100 methane and mix natural gas are compared. However calculated NO_x values compared with the experimental values, mix natural gas reactive analysis results are found closer to the experimental data. For this reason, mix natural gas were used in the other cases.

In the second reactive analyses and experiments which were done with mix natural gas in different burner outputs. Experiments and reactive studies were showed that less than 10 ppm difference occurs between high load and low load when the measured NO_x values compared.

In the third reactive analyses and experiment, mix natural gas composition were used for the second combustion chamber geometry. The difference in NO_x emissions is found to be 2% comparing the experimental results with the numerical solutions. In numerical studies when the measured wall temperature was defined as a wall temperature boundary condition, numerical study results are more accurate to experimental values.

With the modified first burner geometry pressure drop of combustion head was decreased but flame shape is not suitable for a burner application. With the improved second burner geometry, NO_x values were decreased. However new geometry should be modified to improve flame shape.

REFERENCES

- [1] Charles E.B., (2013) The John Zink Hamworthy Combustion Handbook Fundamentals Vol.1, 2nd Edition, CRC Press, Oklahoma
- [2] Riello S.p.A (2001) Forced Draught Burner Handbook, 1st Edition, Riello S.p.A, Legnago
- [3] Basu P., Kefa C., Jestin L. (2000) Boilers and Burners Desig and Theory, 1st Edition, Springer, New York
- [4] Strehlow R.A., (1993) Combustion Fundamentals, 1st Edition, Krieger Pub Co,
- [5] McAllister S., Chen J., Fernandez-Pello A.C., (2011) Fundamentals of Combustion Proceses, 1st Edition, Springer, New York
- [6] Bayrakli İ., UZA E., (2016) ECOSTAR Burner & Combustion Technical Handbook, 2nd Edition Termo Isı A.Ş, Istanbul
- [7] Johnston M., (2009) Incomplete Combustion, Tehnical Services Newsletter 1-800-944-2840, Beaulieu of America
- [8] Bilgin A., (2001) Kazanlarda Baca Gazı Analizlerinin Değerlendirilmesi İç Soğuma Kayıplarının İrdelenmsi, 5. Ulusal Tesisat Mühendisliği Kongresi, TMMOB, İzmir
- [9] Chu H., Stoichiometriic Calculations, National Cheng Kung University Lecture Notes, Tainan City
- [10] Özsarfati R., Marg B.S.Z., Yanma Temelleri ve Brülörler, Denko Isı Kontrol Tekniği A.Ş, Istanbul
- [11] EN 676:2008 Automatic Forced Draught Burners for Gaseous Fuels
- [12] EN 267:2011 Forced Draught Oil Burners - Definitions, Requirements, Testing, Marking
- [13] Zevenhoven R., Kilpinen P., (2002) Control of Pollutants in Flue Gases and Fuel Gases, 2nd Edition
- [14] Determination of emissions from appliances burning oil and gaseous fuels during type-testing Annex-1, 1998, 6th Edition

- [15] Sarlej M., Petr P., Hajek J., Stehlik P. (2007) Computational Support in Experimental Burner Design Optimisation. Applied Thermal Engineering 27 (2007) 2727–2731
- [16] Chacon J., Sala J.M., Blanco J.M., (2006) Investigation on the Design and Optimization of a Low NO_x-CO Emission Burner Both Experimentally and through Computational Fluid Dynamics (CFD) Simulations, Energy & Fuels 2007, 21, 42-58
- [17] Spangelo O., (2004), Experimental and Theoretical Studies of a Low NO_x Swirl Burner, Trondheim EPT 2004:11
- [18] Saripalli R., (2004) Simulation of Combustion and Thermal Flow Inside an Industrial Boiler, University of New Orleans Theses and Dissertations
- [19] Khanafer K., Aithal S.M., (2011) Fluid-dynamic and NO_x Computation in Swirl Burners, International Journal of Heat and Mass Transfer 54 (2011) 5030-5038
- [20] Kadar A.H., (2015) Modelling Turbulent Non-Premixed Combustion in Industrial Furnaces, Master of Science Theses Study, <http://repository.tudelft.nl/>.
- [21] Versteeg H.K., Malalasekera W., (2007) An Introduction to Computational Fluid Dynamics, 2nd Edition, Pearson,
- [22] Fontes C.E., Bacchi R.D.A., (2010) Best Practice Guidelines for Combustion Modeling, 2010 Ansys South American Conference & ESSS Users Meeting, Sao Poula
- [23] Natural Gas Density Calculator,
<http://www.unitrove.com/engineering/tools/gas/natural-gas-density>
- [24] Natural Gas Calorific Value Calculator,
<http://www.unitrove.com/engineering/tools/gas/natural-gas-calorific-value>
- [25] Manak B., Marg B.S.Z., (2003) Bureau of Indian Standards-Natural Gas Calculation of Calorific Values, Density, Relative Density and Wobbe Index from Composition, Printograph, New Delhi
- [26] Manak B., Marg B.S.Z., (2003) Bureau of Indian Standards-Natural Gas Calculation of Compression Factor, Simco Printing Press, Delhi
- [27] Testo Inc, Flue Gas Analysis in Industry, 2nd Edition, Testo Inc., Sparta

- [28] Cleaver Brooks (2010) Boiler Emission Guide, 1st Edition, Cleaver Brooks, Thomasville
- [29] Poinso T., Veynante D., (2001) Theoretical and Numerical Combustion, 1st Edition, Edwards, Philadelphia
- [30] Ansys Inc. (2016) Fluent Combustion Training Notes, 1st Edition, Ansys Inc., Canonsburg
- [31] Hesselmann G., Rivas M., What are the Main NO_x Formation Processes in Combustion Plant, 1st Edition, IFRF Combustion Handbook (<http://www.handbook.ifrf.net>), ISSN 1607-9116
- [32] TSI Inc., (2004) Combustion Analysis Basics, TSI Inc., Minnesota

CURRICULUM VITAE

Engin Uza was born in Istanbul on 17.11.1989. He is an only child of his family. He completed his first five years of primary education at Fındıkzade Primary School and his last three years at Oguzkaan College. He started his university education at Yıldız Technical University Faculty of Naval Architecture and Maritime, Department of Naval Architecture and Marine Engineering after finishing his high school education at Osman Ulkumen High School in 2007. He has been studying his master degree in Marmara University Department of Mechanical Engineering since 2013.

He has been working as a research and development engineer in ECOSTAR Combustion Systems R&D Department for three years.

During his university education, he attended training in Rhinoceros to improve his design and imagination skills. He received education about ANSYS Static Structural and Fluent module to improve his engineering skills. He has attended an Italian language course at the Italian Cultural Center in Istanbul for two years. He attended general English and business English course in Liverpool School of English in United Kingdom.

He is a member of Yıldız Technical University Photography Club.